

The Potential to Generate Exogenic Interneurons for Alzheimer's Disease via  
Blastocyst Complementation

A Thesis SUBMITTED TO THE FACULTY OF THE UNIVERSITY OF  
MINNESOTA BY

Sether Todd Johnson

IN PARTIAL FULFILLMENT OF THE REQUIREMENTS FOR THE DEGREE OF  
MASTER OF STEM CELL BIOLOGY

Adviser: Walter Low, Ph.D.

December 2022

Copyright Sether Todd Johnson, 2022

## ACKNOWLEDGEMENTS

I would like to acknowledge my mentors and examiners including my advisor Dr. Walter Low, Dr. Sue Keirstead, Dr. James Dutton, and Dr. Andrew Grande; all the members of the Low Lab including Dr. Susanne Var, Phoebe Strell, Anala Shetty, and Madison Waldron; other collaborators including Dr. Cliff Steer, Dr. Andrew Crane, and Yun You and the University of Minnesota Mouse Genetics Laboratory; and my friends and family, without whom this work would not have been possible.

## ABSTRACT

Alzheimer's disease (AD) currently affects millions of patients worldwide, and to date the development of effective therapies has been slow. In AD, numerous types of neural cells become dysfunctional and are susceptible to degeneration, leading to cognitive deficits. One particular cell type affected are GABAergic inhibitory interneurons. Normally, these cells function as modulators of neural circuits, and are associated with maintenance of network synchrony and oscillatory signaling important for memory encoding. Impairments in short term memory, electrophysiological abnormalities such as neural hyperactivity and epileptiform spikes, and loss of interneurons are seen in AD patients and AD mouse models. These observations suggest that degeneration and dysfunction of interneurons contributes to cognitive deficits in AD. Thus, restoring interneuron activity is one potential approach to treat AD. The generation of exogenic interneurons via blastocyst complementation is one promising method to generate these cells. In this method, interspecies chimeras are created by genetic editing in a host blastocyst, which establishes a developmental niche to be filled during expansion of the progeny of donor pluripotent stem cells (PSCs) injected into the blastocyst. Blastocyst complementation has several advantages compared to in-vitro directed differentiation of stem cells, namely that development occurs in an in-vivo context. Thus, progenitor cells are exposed to all the inductive cues needed for differentiation to the appropriate cell phenotype of interest, and therefore may more faithfully recapitulate the intended cell-type specific gene networks and biomolecular characteristics of those cells. Studies have shown that this technique can be applied for CNS tissues including specific brain regions. Specifically, previous work from the Low Lab at the University of Minnesota has shown that targeting the homeobox gene *HHEX* establishes a niche for the formation of various organs from donor cells including liver, pancreas, and brain (Ruiz-Estevez et al., 2021). *HHEX* may be a viable target gene for the generation of exogenic interneurons as previous work has indicated that knockout of *HHEX* impairs development of the medial ganglionic eminence (MGE), a developmental structure enriched in GABAergic interneuron

progenitors (Martinez-Barbera et al., 2000). In addition, many studies have demonstrated that engraftment of MGE cells can reduce cognitive and electrophysiological deficits in AD mouse models. This suggests that the transplant of exogenic interneurons may be a feasible strategy to restore interneuron activity and reduce cognitive deficits in AD. While the generation of human-animal brain chimeras is controversial, recent surveys indicate the public is amenable to the concept for research and therapeutic use (Crane et al., 2020). Thus, future translation of this approach using human-porcine chimeras may provide exogenic human interneurons to treat AD patients. This thesis will describe the scientific background and rationale for exogenic interneuron generation by *HHEX* KO/blastocyst complementation as a potential approach to treat AD. It will also show preliminary analysis of *HHEX* KO/complemented mice, and show testing of a primary antibody for Lhx6 in wild type mouse tissue prior to the antibody being used to search for donor-derived interneuron progenitors in chimeras.

## TABLE OF CONTENTS

List of Tables.....	v
List of Figures.....	vi
Introduction.....	1
Methods.....	12
Results.....	24
Discussion.....	32
Bibliography.....	35

LIST OF TABLES

i. Table 1. Apparent chimerism efficiency following *HHEX* KO and  
complementation with PSCs..... 24

## LIST OF FIGURES

i.	Figure 1. Overview of generation of <i>HHEX</i> KO/completed chimeric animals.....	12
ii.	Figure 2. CRISPR/Cas9 construct used in electroporation of zygotes for the generation of <i>HHEX</i> KO mouse embryos.....	14
iii.	Figure 3. Chimerism in ~E12.5 <i>HHEX</i> KO/rESC complemented embryo.....	25
iv.	Figure 4. Results of Lhx6 antibody test 1 in coronal sections of WT E12.5 mouse brain.....	26
v.	Figure 5. Results of Lhx6 antibody test 2 in sagittal sections of WT E12.5 mouse brain.....	28
vi.	Figure 6. Results of Lhx6 antibody test 3 in coronal sections of WT E12.5 mouse brain.....	30
vii.	Figure 7. Hypothesized results of IHC experiments in coronal brain sections of an ~E12.5 chimeric embryo following <i>HHEX</i> KO and complementation with PSCs.....	32



## INTRODUCTION

Alzheimer's disease (AD) is a broadly defined neurodegenerative disorder of the brain which is currently estimated to affect over 6 million Americans over the age of 65<sup>1</sup>. AD is typically characterized by progressive appearance of cognitive deficits with age, the most common of which is memory loss/dementia; however, diagnosis is challenging, as the symptoms and their onset can vary by individual<sup>2</sup>. Impairments in higher order functions are also common and make daily life difficult for afflicted individuals. For example, individuals affected by AD may lack awareness of how and when they traveled to a certain location, experience difficulties with problem solving, planning and judgement, struggle to join or participate in conversations, and confuse events and people<sup>3</sup>. With these challenges, changes in mood are also common, and afflicted individuals can experience anxiety, withdraw from work and social activities, lose interest in hobbies and projects, and exhibit symptoms of depression<sup>3</sup>.

Some of the most common biomolecular pathologies observed in AD are abnormal extracellular accumulation of the peptide amyloid beta ( $A\beta$ ) and intracellular accumulation of tubulin associated unit (tau) proteins<sup>1</sup>.  $A\beta$  peptides vary in length between 40 and 51 amino acids, with the most common being  $A\beta_{40}$  and  $A\beta_{42}$ . These fragments are generated by cleavage of amyloid precursor protein (APP), by beta and gamma secretase enzymes<sup>4</sup>. APP is an integral membrane protein which expressed in neurons, and amyloid proteins normally play a variety of roles including modulating synapses and acting as an innate immune response<sup>5,6</sup>. However, in AD, an excess of  $A\beta$  peptides aggregate extracellularly into oligomers and fibrils. In particular, fibrils accumulate into amyloid plaques, a hallmark of AD which is commonly seen in postmortem examination of patients with dementia, and is to date the benchmark for a definitive AD diagnosis<sup>4,7</sup>. Tau proteins normally assist microtubule assembly and stability, but become hyperphosphorylated and accumulate into large filaments known as neurofibrillary tangles (NFTs)<sup>8,9</sup>. These molecules become widely distributed across the brain in AD, and while exact causative mechanisms remain

to be elucidated, A $\beta$  and tau are associated with inflammation, neuronal toxicity, and brain volume loss<sup>1,10–12</sup>.

Known risk factors for AD include the *APP* gene as well *PSEN1* and *PSEN2*, which encode elements of gamma secretase. These variants lead to greater production of A $\beta$  and have been linked to dementia and early onset/familial AD<sup>13,14</sup>. Early onset AD is rare, making up approximately 5% of all AD cases<sup>13</sup>. The  $\epsilon$ 4 allele of apolipoprotein E (APOE) to date is the main risk factor correlated with late onset AD<sup>13,15</sup>. Late onset AD, also called sporadic or “non-inherited,” makes up the vast majority (95%) of AD cases<sup>13</sup>. There are several proposed theories of how APOE, which normally functions in cholesterol trafficking, contributes to the pathology of AD. One study found that APOE secretion by glia stimulates the production of A $\beta$  by neurons via activation of the MAPK signaling pathway<sup>16</sup>.

More recently, other risk factors have been identified including mutations in the microglial activation gene *TREM2*, other genes such as *C3* and *LUBAC* associated with inflammation, and epigenetic changes such as hypomethylation across the genome<sup>13,17–21</sup>. Despite recent advances in large scale genome wide association studies, much is still unknown about the genetics of AD. Between early and late onset forms, AD has been estimated to have between 60-84% heritability, but less than half can be accounted for by all genetics risk factors currently identified<sup>13,22</sup>. Overall, it appears that most cases of AD are multifactorial, with genetics, age, previous brain injury or infection, exposure to pollution, and comorbidities such as obesity, diabetes, and vascular disease all potentially contributing to cumulative AD risk<sup>1,23</sup>.

The public health burden of AD is significant due to the long duration of illness before death, and includes effects on the afflicted individual, families, and caregivers. The total estimated cost of AD healthcare in 2020 was \$305 billion dollars<sup>24</sup>. As the proportion of the U.S. population 65 and older is projected to grow in future years, the societal cost and burden will grow as the number of existing and novel AD cases will increase as well<sup>1</sup>. These trends make the

development of effective treatments for AD a priority, especially as current best in class therapies may only slow progression of the disease, and some, namely aducanumab, have been subject to controversy regarding their efficacy<sup>10,25–27</sup>.

Irregular signaling and neurodegeneration occurs in many parts of the brain in AD including the hippocampus, entorhinal cortex, nucleus basalis and medial septal nucleus, amygdala, dorsal raphe nucleus, and locus coeruleus<sup>28–40</sup>. One neural cell type which has garnered attention as a potential therapeutic target in AD is inhibitory interneurons.

Generally, interneurons are non-motor, non-sensory neurons which function to modulate neural circuits<sup>41</sup>. They are a heterogenous collection of cells which can be classified into numerous subtypes based on the neurotransmitter they secrete, the expression of specific molecular markers such as parvalbumin (PV) and somatostatin (SST), their electrophysiological properties, and their morphology<sup>42–45</sup>. GABAergic interneurons, which release gamma-aminobutyric acid (GABA) as their neurotransmitter, are widely distributed throughout the mature brain, particularly in the cortex (they make up around 20% of all cortical neurons), cerebellum, hippocampus, and striatum<sup>41,46</sup>. These cells make wide ranging connections, often synapsing on more than one cell, and generally function to inhibit the firing of other neurons<sup>47</sup>. Through broad inhibition of neural activity, they act to modulate neural circuits, maintaining synchronous and oscillatory neural activity<sup>47,48</sup>.

As with other neural cell types, GABAergic interneurons become dysfunctional and are lost in AD. Parvalbumin (PV) and somatostatin (SST)-expressing GABAergic interneurons, among other subtypes, have been observed to be susceptible in AD patients and AD mouse models<sup>48–58</sup>. These deficits are correlated with the appearance of AD pathology, including the deposition of A $\beta$  and tau, and are linked to imbalances in excitatory and inhibitory signaling, widespread hyperactivity, and decreased oscillatory signaling in the gamma range, and epileptic-like spikes<sup>46,48,57–60</sup>. Notably, AD patients appear to have a relatively increased incidence of seizures<sup>61,62</sup>. The loss of oscillatory signaling in

the gamma range, or decrease in gamma power, is significant as gamma signaling is strongly associated with memory processing and encoding<sup>48,63,64</sup>. These findings suggest that a decrease in inhibitory signaling from interneurons has occurred. While the exact pathology is still under investigation, one potential biochemical mechanism for diminishing interneuron function in AD is decreased expression of the voltage gated sodium channel Nav1.1. This protein is primarily expressed in inhibitory interneurons and serves to help initiate the rising of the action potential<sup>65</sup>. Nav1.1 expression is decreased in certain AD mouse models, possibly due to cleavage by beta secretase<sup>50,66,67</sup>. Overall, these observations support the idea that loss of interneuron function and loss of interneurons themselves in AD is tied to cognitive deficits. Thus, restoring interneuron activity and/or interneurons is a potential approach to treat AD.

One treatment approach which has been explored to supplement dysfunctional interneuron activity and replace lost interneurons in AD is cellular therapy, specifically, transplantation of interneuron progenitor cells from the embryonic medial ganglionic eminence (MGE). The MGE is a forebrain structure which is present transiently in development and is especially prominent at embryonic day 12.5 (E12.5). It is well established that between 60-70% of GABAergic interneurons derive from progenitor cells in the MGE, especially PV and SST-expressing interneurons<sup>68-70</sup>. The MGE is well defined morphologically, and can also be identified by the expression patterns of numerous early and late-expressing transcription factors, including Nkx2.1, Lhx6 and Lhx8, and Dlx1 and Dlx2<sup>68,69,71</sup>. Characteristics of MGE progenitor cells which make them attractive candidates for cellular therapy include their capacity to survive, migrate long distances, and differentiate into various types of morphologically and functionally mature interneuron subtypes<sup>70,72-80</sup>. For example, in 2006, Alvarez-Dolado et al. observed that MGE cells transplanted into the cortex differentiated within one month into bipolar cells, chandelier cells, basket cells, and multipolar cells, and MGE cells transplanted into the hippocampus differentiated into basket cells, axo-axonic, and bipolar cells. All these observations matched the cell types and distribution which is stereotypic to that region in normal brain tissue<sup>70</sup>.

Transplanted MGE cells also appear able to integrate into existing neural circuitry, both *in-vitro* in brain slices and after transplantation into a host animal<sup>70,72–80</sup>. Transplant of the MGE has been explored in pre-clinical animal models as a treatment for disorders of the central nervous system (CNS) including schizophrenia<sup>81–83</sup>, hearing loss<sup>84</sup>, Parkinson's disease<sup>85</sup>, epilepsy<sup>78,86–93</sup>, neuropathic pain<sup>94</sup>, autism<sup>95</sup>, and traumatic brain injury<sup>96</sup>.

Several studies have investigated MGE transplant for AD<sup>67,97,98</sup>. In 2014, Tong et al. transplanted MGE cells into apoE4 knock-in and APP mice, which develop GABAergic interneuron dysfunction and memory deficits<sup>50,99,100</sup>. Grafted cells survived for 90+ days post-transplant and matured into primarily SST-expressing interneurons. Electrophysiological recordings indicated an increase in spontaneous inhibitory post-synaptic potentials in hippocampal cells, which was correlated with a degree of improvement in cognitive function and memory tests<sup>97</sup>. Importantly, the authors also transplanted MGE cells into a cohort of apoE3 knock-in mice, which do not have memory defects, and observed no differences in cognitive function between transplanted and non-transplanted cohorts<sup>97</sup>. This was interpreted as a sign that while MGE transplants could improve cognition in recipients with diseased brains, they did not introduce abnormalities in normal brains. In a 2022 paper, Lu et al. tested MGE transplant in APP/PS1 mice, which lose GABAergic interneurons and develop memory deficits, and observed similar improvements in learning and memory. They also reported a decrease in epileptic spikes and an apparent increase in long term potentiation measured by an increase in synapse strength in response to high-frequency excitation<sup>98</sup>. Finally, Martinez-Losa et al. in 2018 investigated the possibility of adjusting the biomolecular characteristics of MGE cells to optimize their efficacy. Interestingly, transplant of Nav1.1-overexpressing, but not wild type MGE, led to improved cognition in an APP mouse model, in contrast to other studies<sup>67</sup>. The authors speculate that this result may have been due to differences in mouse models, as their model develops interneuron dysfunction without significant cell loss. Importantly, in these studies, the transplanted cells

survived and did not appear to be affected by the existing AD-like pathology in the transgenic mouse models.

While the relative safety and efficacy of MGE transplant for neurological diseases including AD has been validated in animal models, there are ethical, moral, and legal barriers to the use of embryonic human tissue as a therapy. One potential solution is the derivation of MGE-like cells from human pluripotent stem cells (PSCs) *in-vitro*. Several protocols have been published describing the generation and culture of MGE-like cells<sup>101–106</sup>, and some studies have investigated their transplant in animal models of disease<sup>107–110</sup>. However, this approach has several limitations, most significantly, the fact that cells grown in culture may not accurately represent the *in-vivo* cellular phenotype. For example, in 2016, Ahn et al. reported that after transplant of human ESC-derived MGE-like cells into the hippocampus of a mouse, at 4 months post-transplant approximately 30% of the transplanted cells were SST+ and approximately 8% were PV+<sup>102</sup>. In comparison, Alvarez-Dolado et al. in 2006 reported that of all freshly dissected mouse MGE cells transplanted into mouse hippocampus, approximately 34% were SST+ and 34% were PV+ at 60 days post-transplant<sup>70</sup>. These results suggest that cultured, PSC-derived MGE-like cells may have different differentiation capacity than *in-vivo* MGE cells. Traditional culture systems lack the three-dimensional structure of a developing animal, and while improvements have been made with the advent of “organ on a chip” and organoid systems, these cannot provide the complete, *in-vivo* biomolecular context. This context includes but is not limited to a complex morphogen environment, cell-cell contact and activation of intracellular signaling pathways, transcription factor activity, and mechanical forces, all of which occur at specific quantities and are coordinated in time and space.

One method which bypasses the limitations of *in-vitro* culture and may allow the generation of exogenic interneuron progenitor cells which accurately reflect their *in-vivo* phenotype is interspecies blastocyst complementation. Blastocyst complementation involves the addition of donor PSCs to an early-stage host

embryo which has been genetically engineered to lack development of a specific organ or tissue<sup>111,112</sup>. Complementation with pluripotent donor cells from a different individual produces a chimera, or an animal composed of tissues from multiple sources, deriving its name from the Greek myth of a monster with the body of a lion, the head of a goat, and the tail of a snake. Chimeras contain populations of genetically unique cells within the same organism. A primary or systemic chimera will have genetically unique cells in most or all tissues, while in a secondary or partial chimera genetically unique cells may contribute to one or a few tissues. Systemic chimeras can be generated if the unique cells were combined in early embryogenesis, and partial chimeras are typically generated when combination occurs later in development<sup>113</sup>. If the sources of the contributing cells are different individuals of the same species, the chimera is referred to as intraspecies; if the two sources are individuals of different species, the result is an interspecies chimera.

Chimeras have been used to study biology and disease for decades and have been particularly useful to study development<sup>113-116</sup>. One of the first reports of an intraspecies mouse chimera was in 1961, accomplished via fusion of two partial embryos<sup>117</sup>. A little over ten years later, the first mouse-rat interspecies chimeras were generated by isolation of the inner cell mass from a E4.5 rat embryo, which was inserted into the blastocoel of an E3.5 mouse embryo<sup>118</sup>. This technique forms the basis of blastocyst complementation. However, in blastocyst complementation, ablation of a target gene essential to the development of a specific organ or tissue is performed in the host prior to insertion of donor PSCs. This creates a "niche" to be filled by donor cells and their progeny, as if ablation of the target gene in the host is complete, donor-derived cells which do possess the target gene should be the only cells capable of contributing to the formation of that organ or tissue. Thus, the target organ or tissue in the resulting chimera may be nearly 100% donor derived. Today, gene knockouts (KO) can be performed with relatively high efficiency via CRISPR-Cas9-mediated gene editing at the zygote stage<sup>111</sup>. Labeling of the donor cells, typically accomplished with

fluorescent markers such as green fluorescent protein (GFP), allows donor cells to be tracked<sup>111,119</sup>.

One of the first studies applying blastocyst complementation was published by Chen et al. in 1993. Mouse embryos deficient in Rag2, normally unable to produce mature T and B lymphocytes, were injected with ES cells, producing chimeric animals with functioning immune systems<sup>4</sup>. Modifying the injected ES cells allowed investigation of which genes were necessary for lymphocyte development. Thus, one application of blastocyst complementation was for study of developmental biology. This approach was subsequently used in further studies of T and B cell development<sup>120–124</sup> as well as the development of the ocular lens<sup>125</sup> and thymus vasculature<sup>126</sup> through targeting of other tissue and organ-specific genes.

More recently, blastocyst complementation has been explored as a way to generate exogenic tissues for transplantation. Pioneers in this field include Hiromitsu Nakauchi and Jun Wu, whose groups have published papers since the early 2010s characterizing the generation of a variety of cells, tissues, and organs. These groups and others have reported generation of exogenic pancreas, liver, heart, kidneys, lungs, vasculature, and eye, as well as methods to overcome challenges associated with blastocyst complementation, particularly mechanisms leading to death of donor cells including competition with the host<sup>111,112,127–132</sup>. Notably, generation of CNS tissues has been reported. In 2018, Chang et al. described “neural blastocyst complementation,” in which targeting the gene *Emx1* led to ablation of dorsal telencephalic neurons<sup>133,134</sup>, and in 2021, Steevens et al. reported generation of inner ear sensory neurons<sup>135</sup>. These studies demonstrated that blastocyst complementation could be applied to the CNS, and even to specific brain regions, as Chang et al. reported a chimeric brain with donor-derived forebrain.

Recent published and unpublished work from the Low Lab at the University of Minnesota investigated blastocyst complementation targeting the gene *HHEX*. The Hhex protein is a homeobox transcription factor which regulates the



development of a number of organs, including the liver, pancreas, heart, and bile duct<sup>119,136,137</sup>. Knocking out the *HHEX* gene followed by blastocyst complementation led to donor cell contribution in the liver, pancreas, and brain<sup>119</sup>. Other groups have also investigated *Hhex* as a possible target for blastocyst complementation<sup>131</sup>. The creation of a niche in the brain following *Hhex* blastocyst complementation is plausible, as Martinez-Barbera et al. (2000) observed defects in forebrain development in *HHEX*<sup>-/-</sup> mutant embryos. Specifically, they observed reduced size or complete loss of telencephalic vesicles, from which the medial ganglionic eminence (MGE) derives, and disrupted expression patterns of key factors regulating interneuron development, including *Nkx2.1*, *Pax6*, and *Fgf8*<sup>138</sup>. Given the importance of these regions and genes in early interneuron specification, the observation that loss of *Hhex* results in impaired MGE development with reduced *Nkx2.1* expression suggests that *HHEX* KO may impair the generation of interneurons. Thus, targeting *HHEX* for genetic ablation may provide a niche for the generation of donor-derived interneurons in blastocyst-complemented chimeras.

When considering interneuron progenitor cell therapy, there are several advantages to a blastocyst complementation MGE graft approach. The main benefit to using blastocyst complementation over in-vitro derivation of interneuron progenitors is that the cells develop with full, in-vivo context, as described earlier. Therefore, cells generated via blastocyst complementation may more faithfully recapitulate the intended phenotype and biomolecular characteristics. This has been observed in MGE transplant studies – cells from MGE grafts migrate long distances and acquire mature morphology, in contrast to embryonic stem cell (ESC)-derived neurons and cells genetically engineered to produce GABA<sup>70</sup>. Importantly, control of these characteristics appears to be sufficiently cell-autonomous, as MGE cells transplanted into adult brains retain their migratory and differentiation potential, despite a mismatch in age<sup>75</sup>. MGE cells are also able to engraft and survive in disease-state environments, such as mouse models of AD whose brains overexpress toxic A $\beta$  and tau<sup>97,98</sup>. These results are

promising as they suggest that cells transplanted in human AD patients may be able to survive and contribute to cognitive improvements.

In the future, blastocyst complementation with *HHEX* KO to generate MGE for treatment of AD in human patients would likely involve the creation of human-pig chimeras. Pigs have previously been explored as host animals for the generation of exogenic tissue including liver and pancreas due to their greater similarity to humans versus rodents<sup>111,119,128,131</sup>. The size of porcine organs and cells is more similar to humans compared to rodents. There is also greater genetic overlap between pigs and humans, as these species diverged more recently than rodents and humans. This greater genetic overlap improves the efficiency of chimerism<sup>111,129,139</sup>. A recent study by Casalia et al. in 2021 found that GABAergic interneurons develop from an MGE in pigs as in rodents, supporting the potential to generate a donor-derived MGE in pigs<sup>140</sup>. However, the generation of chimeric animals which include contribution of human cells to the brain is a subject of controversy. Guidelines on the use of human stem cells in chimera research have been established by various organizations, including the International Society for Stem Cell Research (ISSCR) and National Institutes of Health (NIH). Additional oversight is suggested for studies that involve potential contribution of human cells to the CNS or germline, and researchers are proceeding with caution<sup>114,141</sup>. One concern about the creation of chimera with human brain cells is “humanization” of the animal. A few studies have investigated transplant of human neural cells into adult animals. Human cells appear to functionally integrate into mouse neural circuits<sup>142</sup>, and one study even observed apparent improvements in cognitive function after grafting of human glial progenitor cells<sup>143</sup>. This and other studies were reviewed by Crane et al. (2019), and out of 150 instances of transplantation of human cells into animal brains, little evidence of “human-like” cognition or behavior was observed<sup>144</sup>. Studies which involve the combination of human stem cells and animal embryos, while not illegal, are currently prohibited from receiving NIH funding<sup>141</sup>. However, recent surveys indicate that the use of human-animal chimeras for research and therapeutic transplantation, even those which include contribution to the brain,

had a degree of support from various components of the U.S. population. In 2020, Crane et al. reported that roughly 59% of the U.S. public could accept the use of hiPSC in human into pig blastocyst complementation and the transplant of human organs from the resulting chimeras<sup>145</sup>. Therefore, future translation of blastocyst complementation-generated interneuron transplant remains an avenue worth investigating.

The hypothesis tested in this research was that targeting the gene *HHEX* will create a niche for the generation of donor-cell derived interneurons. The practical goal was to analyze tissue from chimeric embryos to apply immunohistochemistry (IHC) with fluorescent antibodies and microscopy to provide evidence that the embryos contained interneuron progenitors derived from donor PSCs. Briefly, *HHEX* KO mouse embryos were generated by microinjection of CRISPR-Cas9 targeting *HHEX*. Enhanced green fluorescent protein (eGFP) expressing rat ESCs (rESCs) were injected into the developing blastocyst at approximately E3. Chimeric embryos were then transferred to pseudopregnant host mouse mothers and allowed to develop for approximately 12 days. On approximately E12.5, host mothers were sacrificed, and chimeric embryos were cryopreserved. Embryos were then sectioned and stained with Lhx6 and DAPI to identify interneuron progenitors in the MGE. The scope of this study was to analyze interspecies and intraspecies chimeras generated using *HHEX* blastocyst complementation. To this end, preliminary analysis of *HHEX* blastocyst complemented chimeras was performed, and experiments were done to validate specific staining of an Lhx6 primary antibody in wild type mouse tissue, prior to the antibody being used to search for donor-derived MGE in chimeras.

## METHODS

The goal of this project was to investigate whether blastocyst complementation with *HHEX* KO would allow the generation of donor derived-interneuron progenitors in chimeric mice. The overall project protocol is summarized in Figure 1.

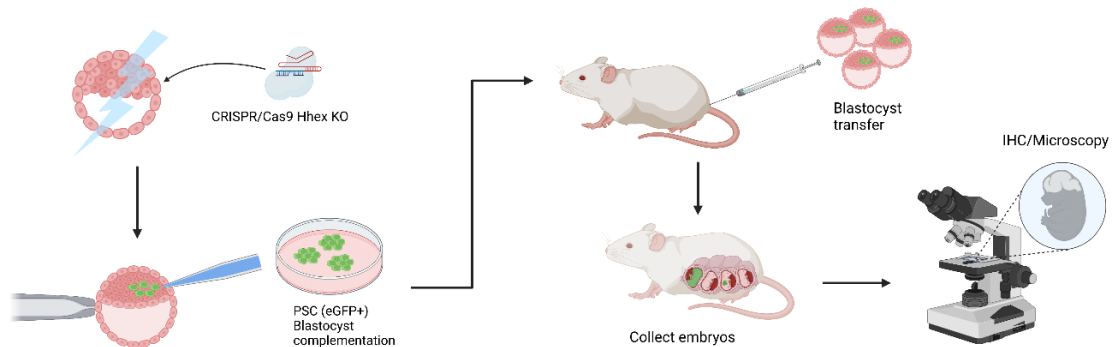


Figure 1. Overview of generation of *HHEX* KO/completed chimeric animals. PSCs used included rESC or miSPC, which were injected into mouse blastocysts and transferred into host female mice to produce interspecies and intraspecies chimeras. Produced using Biorender.com.

## ANIMALS

All research procedures involving mice were subject to approval by the University of Minnesota Institutional Animal Care and Use Committee (1910-37539A). Mice were housed in individual micro-isolator cages with Enviro-Dri bedding (Shepherd Specialty Papers) on a light:dark cycle of 12 hours:12 hours with lights turned on at 7:00am. Mouse strains used included female C57BL6 mice and C57BLS/J stud male mice (Jackson Laboratory).

## BLASTOCYST COLLECTION

To create *HHEX* KO zygotes, wild type (WT) mouse zygotes were isolated as previously described<sup>119</sup> by the author and other members of the Low Lab. Mouse zygotes were isolated from females which were induced to super-ovulate by intraperitoneal injection in the lower left abdomen of 5 IU human chorionic gonadotropin (hCG). This was performed to induce a greater number of eggs relative to a normal ovulation event. After super-ovulation, females were placed

in the same cage as stud males for mating. The next day, female mice were observed for the presence of a vaginal plug indicating successful copulation. For reference, the presence of a vaginal plug was considered approximately E0.5, approximately 12 hours after conception. Mice with a plug were removed from their cage and were sacrificed using cervical dislocation. The bilateral ovary, oviduct, and proximal uterine horn were dissected and placed in modified Human Tubal Fluid media (mHTF)<sup>146</sup> in sterile Petri dishes. Zygotes were dissected and placed in sterile Petri dishes in 500  $\mu$ L of 0.3 mg/mL hyaluronidase diluted in 3 mL mHTF. The Petri dishes containing the zygotes were then placed in an incubator at 37°C, 5% CO<sub>2</sub> for 2 minutes. Hyaluronidase is an enzyme that degrades hyaluronic acid (HA), a component of the extracellular matrix. This was performed to isolate oocyte cells from the cumulus cells, which normally surround a fertilized oocyte, and therefore improve the efficiency of CRISPR-Cas entry in the next step.<sup>119,147</sup>

## GENE EDITING

After the isolation of WT zygotes, they were edited using a CRISPR-Cas construct to knock out *HHEX*. This was done in order to generate a hypothetical niche to be filled by donor PSCs expressing Hhex protein. CRISPR (an acronym for **clustered regularly interspaced short palindromic repeats**) refers to a genetic system observed in bacteria which consists of short DNA sequences corresponding to DNA sequences found in viruses. Cas (CRISPR-associated protein) refers to a family of endonucleases, enzymes which create double-stranded breaks in DNA. In bacteria, these components act in tandem as a type of adaptive immune system. During a viral infection, viral DNA sequences are “acquired” by the bacteria and integrated as short sequences called spacers into a specific region of the bacterial genome (the CRISPR locus) adjacent to sequences encoding Cas proteins. When transcribed into RNA, these spacers form complexes with Cas proteins, and the complex is guided to the corresponding sequences in the viral genome via complementary base pairing. This leads to targeted activity of the endonuclease and cleavage and degradation

of the viral DNA. These systems have been adapted for high-specificity genetic editing.<sup>148–154</sup> The CRISPR-Cas9 construct used to generate *HHEX* KO embryos in this study consisted of tracrRNA duplexed with mmHHEX guide RNA, sequence CCACAGGCAAGCCCUUGCUC (Synthego) and Cas9 (#1081060, Integrated DNA Technologies). This construct (Figure 2) was previously designed, validated to successfully knockout *HHEX*, and validated for use in blastocyst complementation by the Low Lab.<sup>119</sup>

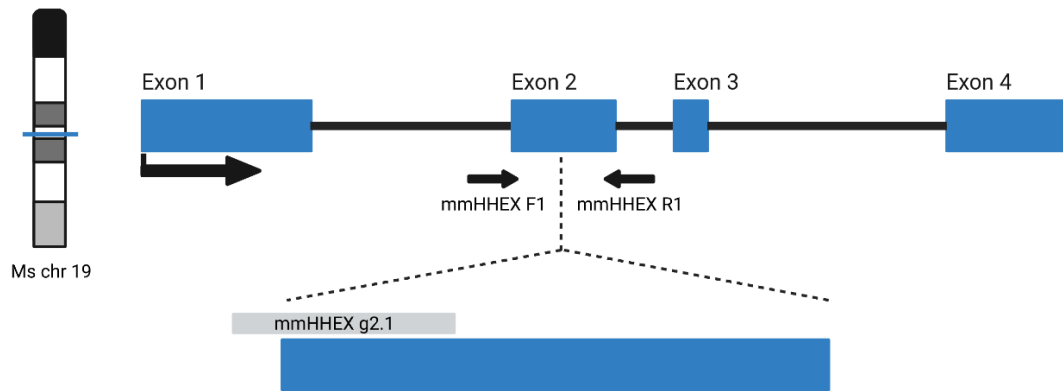


Figure 2. CRISPR/Cas9 construct used in electroporation of zygotes for the generation of *HHEX* KO mouse embryos. Modified from Ruiz-Estevéz et al. (2021), produced using BioRender.com.

Entry of the CRISPR-Cas construct into the zygotes was accomplished via electroporation. This step was performed as previously described<sup>119</sup> in collaboration with the University of Minnesota Mouse Genetics Laboratory (MGL). Electroporation involves the application of an electric field to cells in order to create an electric potential within the lipid bilayer of the cell membrane. After the induced potential surpasses the intrinsic dielectric strength of the membrane, the lipids reorient themselves with the induced field, disrupting the membrane and creating pores. This allows large, impermeable molecules such as CRISPR-Cas, which would typically be unable to pass through the membrane, to enter the cytoplasm, after which they can be trafficked through the cell and imported into the nucleus<sup>155</sup>. After incubation in dilute hyaluronidase, zygotes were washed in Opti-MEM (Thermo Fisher Scientific) twice before being added to a 1-millimeter electroporation cuvette with tracrRNA with *HHEX* guide RNA2.1 at 250 ng/ $\mu$ L,

Cas9 at 250 ng/ $\mu$ L, and Opti-Mem in a final volume of 20  $\mu$ L pre-chilled to 4°C. The electroporation machine used was the Gene Pulser Xcell (Bio-Rad). The parameters used were 2 square wave pulses at 30 volts, duration 3-milliseconds, with a 100-millisecond interval. Zygotes were then removed from the cuvette, washed twice in mHFT, and moved to a drop of mHFT under mineral oil for culture. This process, including the concentrations of CRISPR and Cas reagents and the electroporation parameters, was previously used to generate *HHEX* KO zygotes for blastocyst complementation<sup>119</sup>. Electroporated zygotes were incubated at 37°C, 5% CO<sub>2</sub> for approximately 72 hours, at which point they had reached the blastocyst stage at approximately E3.5.

#### RAT EMBRYONIC STEM CELLS

The cells used for rat into mouse interspecific complementation were eGFP-labeled rat embryonic stem cells (rESCs) (rat strain RRRC: 654 - F344-Tg (UBC-EGFP)F455Rrrc-ES4011/Rrrc, RGD, Milwaukee, WI)<sup>156</sup>. These cells were previously validated to express eGFP, which was inserted on chromosome 5 and driven by the ubiquitin C promoter. The protein is expressed in the cytoplasm and green fluorescence can be visualized throughout the cell. The rESCs were maintained in culture at 37°C, 5% CO<sub>2</sub> on a feeder layer of irradiated mouse embryonic fibroblasts (MEFs) (#PSC001, R&D Systems). Co-culture of PSCs with MEFs promotes maintenance of pluripotency and survival of the stem cells by emulating the in-vivo stem cell niche. MEFs and other fibroblast lines are often referred to as “support” and “feeder” cells. They provide extracellular matrix to which stem cells adhere and secrete factors such as leukemia inhibitory factor (LIF) that inhibit differentiation<sup>157,158</sup>. Culture flasks were plated with MEFs one day prior to addition of the PSCs. The media used for rESC culture was N2B27 + 2i, prepared according to the instructions for rESC culture from the Rat Resource & Research Center (Columbia, MO). 1mL of N2 (Gibco) solution was then mixed with 100 mL DMEM/F12, and this solution was combined with a mixture of 100 mL Neurobasal media (Invitrogen) and 2 mL B27 (Invitrogen). 0.1%  $\beta$ -mercaptoethanol and 2 inhibitors were then added: CHIR99021 (3  $\mu$ M) and

PD0325901 (0.5  $\mu$ M). These small molecules inhibit the Wnt and Mek/Erk signaling pathways, respectively, with the overall effect of promoting the maintenance of pluripotency<sup>159</sup>. After plating rESCs, the N2B27 + 2i media was changed daily, with passaging every 48-72 hours. Passaging was performed as follows: rESC colonies were detached from MEF feeders by gentle pipetting up and down and collected in a 15 mL conical tube. 1X Accutase Cell Dissociation Reagent (Stem Cell Technologies ) was then added to the tubes, which were placed in an incubator at 37°C, 5% CO<sub>2</sub> for 5 minutes. Accutase contains enzymes including collagenases which break up the extracellular matrix connecting cells<sup>160</sup>, allowing for the creation of a single cell suspension. This is necessary in order to dilute the cells and replate on a new flask at a lower density. If PSCs become overconfluent in culture, cell death can occur due to competition for nutrients, oxygen, and space. Overconfluent cultures can also display spontaneous differentiation; thus, passaging is necessary to maintain cell health and pluripotency.

#### MOUSE INDUCED PLURIPOTENT STEM CELLS

The cells used for mouse intraspecific complementation were eGFP-labeled mouse induced pluripotent stem cells (miPSCs) (UMN-3F10)<sup>161</sup>. These cells were previously validated to express eGFP, which is expressed as a transmembrane protein<sup>161</sup>. These cells have also previously been used in successful blastocyst complementation experiments<sup>119</sup>. The miPSCs were maintained in culture at 37°C, 5% CO<sub>2</sub> in a co-culture with irradiated MEFs. The media used for miPSC culture contained KnockOut DMEM with 4.5 g/L sodium pyruvate and D-glucose (ThermoFisher Scientific), 10% fetal bovine serum (FBS) (HyClone), 10% Gibco Knockout serum replacement (ThermoFisher Scientific), 1X Gibco GlutaMAX (ThermoFisher Scientific), 1X Gibco MEM non-essential amino acids (ThermoFisher Scientific), 1X Corning penicillin/streptomycin (ThermoFisher Scientific), 1,000 U/mL ESGRO-LIF (Millipore Sigma), and 0.1mM 2-mercaptoethanol (ThermoFisher Scientific). After plating, the miPSC media was changed daily, with passaging every 48-72 hours. Passaging was performed



as with rESCs, with the substitution of approximately 0.25% trypsin (Gibco) for Accutase.

## BLASTOCYST COMPLEMENTATION AND TRANSFER

After the *HHEX* KO blastocysts had been generated, blastocyst complementation with PSC lines was performed as previously described<sup>119</sup> in collaboration with the University of Minnesota MGL. PSCs (both rESCs and miPSCs) were collected and prepared for blastocyst complementation. Cells were collected approximately between passage 19 and 30. To prepare the PSCs, their culture was washed in 1X phosphate buffered saline (PBS) lacking calcium and magnesium to remove culture media. After washing, either 1X Accutase (for rESCs) or 0.25% trypsin (miPSCs) was added to culture dishes, which were placed in an incubator at 37°C, 5% CO<sub>2</sub> for 5 minutes. This step was performed to create a single cell suspension, so that later individual cells could be injected into blastocysts. After incubation with Accutase or trypsin, the solution of dissociated cells was diluted with their respective culture media, transferred to a 10 mL tube, and centrifuged at 328g for 5 minutes. Then, 5 mL of PBS was added to the tube and the cells were resuspended by gentle pipetting and inversion of the tube. The cells were then centrifuged at 328g for 3 minutes, and afterwards resuspended in their respective culture media. These steps were performed to fully breakup extracellular matrix connections and as preparation for removal of the MEFs. After the centrifugation steps, the cell suspension was transferred to a T75 flask treated with gelatin and placed in an incubator for 1.5 hours at 37°C, 5% CO<sub>2</sub>. This step was performed to separate the MEFs from the PSCs, as in a short period of culture, fibroblasts adhere to the gelatin coating, while PSCs remain in suspension. After separation of the PSCs from the MEFs, the cells remaining in suspension were transferred to a 10 mL tube and centrifuged at 328g for 5 minutes. After centrifugation, the supernatant was removed, and the pelleted PSCs were resuspended in approximately 1 mL of culture media in a 1.7 mL micro-centrifuge tube. From there, the prepared PSCs were placed on ice and

transported to the site of the blastocyst complementation step, where they were injected within 2 hours of preparation.

Prepared PSCs were suspended in EmbryoMax M2 media (Millipore Sigma) with the ~E3.5 blastocysts. Approximately 10 cells were taken up in a micropipette and injected into the blastocoel cavity, close to the inner cell mass. After the injection, blastocysts were placed in drops of mHFT under mineral oil and incubated at 37°C, 5% CO<sub>2</sub>. After 2-4 hours of incubation, blastocysts were transferred into the uteri of pseudo-pregnant CD1 female mice (Charles River Laboratories) in collaboration with the University of Minnesota MGL.

Pseudopregnant mice were created as follows: approximately 4.5 days prior to blastocyst transfer, CD1 female mice were mated with vasectomized CD1 male mice. After mating, female mice were observed for the presence of a vaginal plug, which indicated approximately E0.5. Two days after observation of plugs, pseudo-pregnant female mice were anesthetized with 225 mg/kg Avertin, and blastocyst transfer was performed. Female mice were returned to individual cages and observed until the determined timepoint for embryo extraction.

## EMBRYO COLLECTION AND PRESERVATION

In this study, complemented and WT embryos were extracted as previously described<sup>119</sup> and analyzed at approximately E12.5. This timepoint is during the period in which the MGE transiently forms during development, and during a period of robust *Lhx6* expression in MGE interneuron progenitors<sup>162–164</sup>. On the day of embryo extraction, pregnant females were asphyxiated with CO<sub>2</sub> and euthanized by cervical dislocation. The uteri were dissected and transferred to sterile Petri dishes filled with PBS on ice. Embryos were dissected from the uteri and transferred to a 50 mL tube in PBS on ice and transported from the University of Minnesota MGL to the Walter Low Lab for fixation.

Less than 2 hours after extraction, embryos were transferred to a 12 well plate and approximately 2-4 mL of 4% paraformaldehyde (PFA) was added to the wells. Embryos were incubated in 4% PFA at 4°C for no more than 24 hours. PFA forms crosslinks between proteins, preventing decay and preserving the

structure of the embryo for later analysis. After fixation with PFA, the PFA was removed from the 12 well plate using a pipette. Embryos were washed by adding approximately 2-4 mL of PBS . After 5 min, PBS was removed, and approximately 2-4 mL of a solution of 10% sucrose in PBS was added to the well plate. Embryos were incubated in 10% sucrose at 4°C for approximately 24 hours. Then, 10% sucrose was removed, and approximately 2-4 mL of a solution of 20% sucrose in PBS was added to the well plate. Embryos were incubated in 20% sucrose at 4°C for 24 hours. After 24 hours, the 20% sucrose was removed from the well plate, and approximately 2-4 mL of a solution of 30% sucrose in PBS was added. Embryos were again incubated for 24 hours at 4°C. Embryos were considered to be fixed when they settled at the bottom of the well plate after incubation in 30% sucrose. Incubation in increasing concentrations of sucrose was performed in order to promote dehydration of the tissue. When placed in the sucrose solutions, water will leave the tissue through the skin to the solution of higher solute concentration. This step was performed to prepare the tissue for freezing, as dehydrating the tissue prevents the formation of ice crystals.

#### CRYOSECTIONING

After completion of the fixation protocol, embryos were removed from 12 well plates using a forceps and gently blotted dry with a KimWipe (Science KimTech). Embryos were then suspended in optimal cutting temperature (OCT) media (Fisher Healthcare) in plastic cuvettes, and frozen by placing the cuvette over dry ice. Frozen embryos were stored at -80°C prior to cryosectioning. Frozen embryos were sectioned at thickness between 14-20 µm using a Leica CM1850 cryostat. Sections were placed on Fisherbrand Superfrost Plus slides (Fisher Scientific), with 2-5 sections per slide. Slides were warmed to approximately 40°C on a heat block for no longer than 30 minutes after sectioning, and then transferred to a slide box and stored at -20°C prior to immunohistochemistry (IHC) staining. Sections in both the coronal and sagittal planes were collected.

## GENOTYPING

Genotyping was performed with the intent to assess whether the CRISPR-Cas KO of *HHEX* was successful. Tissue samples which were collected for genotyping include: E4.5 blastocysts (after *HHEX* KO, to test CRISPR-Cas electroporation process), a section of the tail collected during initial embryo extraction, or 3-5 cryosections. For tail tip samples, a genomic DNA extraction kit was used prior to WGA, and for cryosections, a formalin-fixed paraffin-embedded (FFPE) DNA extraction kit was used. These steps were performed to increase recovery of DNA from tissue and preserved tissue, respectively. A QIAGEN REPLI-g mini kit was then used for whole genome amplification (WGA) to increase the yield of DNA and optimize later analysis by sequencing. The concentrations of extracted and amplified gDNA were assessed using a Nanodrop Spectrophotometer. Then, PCR amplification and purification of the *HHEX* gene was performed, using forward primer 5'-GCTGGTCTGGGTGGTAGAAC-3' and reverse primer 5'-AGAAAGTCCCAAATCCCGGG-3'. These steps, including primer design, had been previously validated for *HHEX* genotyping<sup>119</sup>. Finally, 75 ng of purified PCR product with 2 µL forward primer in a final volume of 10 µL of water was submitted to Eurofins Genomics for Sanger sequencing. Sequencing results were analyzed using the online Synthego ICE analysis tool.

## IMMUNOHISTOCHEMISTRY

On the day of IHC, slides were warmed at approximately 40°C on a heat block for no longer than 30 minutes. Thawed slides were post-fixed by pipetting approximately 300 µL of 4% PFA on each slide, which were left for 5 minutes. After post-fixing, 4% PFA was removed by gently tipping the slide onto a paper towel. Approximately 300 µL of PBST (0.1% Triton X-100 buffer in PBS) was pipetted onto slides, which were left for 5 minutes, as a wash step. The wash step was repeated three times to remove any 4% PFA. Next, antigen retrieval was performed. This step breaks the cross linkages formed by fixation in PFA through a combination of heat and application to a weak acid, exposing antigenic

sites<sup>165</sup>. A solution of 10 mM sodium citrate and 0.05% Tween 20 at pH 6 was prepared, added to a Coplin jar, and boiled in a microwave. Slides were then placed in the Coplin jar, which was transferred to a rice steamer to maintain temperature just below boiling. The slides were steamed for approximately 20 minutes, after which the Coplin jar was removed from the steamer, covered, and left to cool to room temperature.

After antigen retrieval, slides were washed 3 times in PBST for 5 minutes. After the last wash, PBST was gently tipped off the slides, and approximately 300  $\mu$ L of blocking solution was added to each slide. Blocking solution contained 1% BSA and 0.1% Tween 20 in PBS. This step was performed to reduce background fluorescence, as the albumin can bind non-specifically to sites in the tissue. Thus, fluorescent antibodies applied later are not able to bind to those sites occupied by the serum components. Slides were placed in a humid chamber, covered, and blocked for 1 hour at room temperature. Blocking solution was then gently tipped off the slides, and slides were washed 1 time in PBST for 5 minutes. Then, approximately 300  $\mu$ L of a solution of primary antibody diluted in blocking solution was added to each slide. The primary antibody was tested at dilutions of 1:50, 1:150, and 1:500 according to the manufacturer's recommended range. The main primary antibody used in this study was for Lhx6 (sc-271433, Santa Cruz Biotechnology). This antibody is a mouse IgG monoclonal antibody which detects mouse, rat, and human Lhx6 and has been previously validated and used to detect Lhx6 in mouse brain in several recent publications<sup>166–169</sup>. After addition of primary antibody solution, slides were placed in a humid chamber, covered, and incubated at either 4°C overnight or at room temperature for 2 hours. After incubation with primary antibody, the antibody solution was gently tipped off, and the slides were washed 3-5 times in PBST for 5 minutes. A solution of secondary antibody in blocking solution was prepared and passed through a 0.22  $\mu$ m Millex filter (Millipore) to break up any polymerization of the antibody. The secondary antibody solution, as well as the slides from this point on, were kept covered as light exposure can diminish the fluorescence of the antibody. Approximately 300  $\mu$ L of secondary antibody

solution was added to each slide. The main secondary antibody used in this study was a donkey anti-mouse IgG 555 (AbCam). This means it was raised in donkey against mouse IgG, and should bind the mouse IgG anti-Lhx6 antibody and fluoresce at 555 nm. This wavelength was chosen to avoid overlap with the eGFP expressed in the donor PSCs, which display green fluorescence at an excitation wavelength of around 488 nm. Slides were incubated with secondary antibody for no more than 2 hours at room temperature, after which the secondary antibody solution was gently dipped off and the slides were washed 3-5 times in PBST for 5 minutes. Approximately 300  $\mu$ L of a solution of 4',6-diamidino-2-phenylindole (DAPI) diluted 1:1000 in PBS was added to slides, which were covered and incubated for approximately 10 minutes. DAPI specifically binds to DNA of cells and can be excited to emit blue light around 460 nm, and is used to identify the cell nucleus<sup>170</sup>. After staining with DAPI, the solution was gently dipped off and the slides were washed 3-5 times in PBST for 5 minutes. Stained slides were either stored "wet" by placing them in a Coplin jar filled with PBS, or mounted. For mounting, slides were allowed to dry slightly before 2-3 drops of Shandon Immuno-Mount solution (Thermo Scientific) were added to each slide, and a No 1.0 coverslip (Kemtech) was gently lowered onto the slide. Slides in "wet" storage and mounted slides were protected from light and stored at 4°C prior to imaging.

The IHC process was first performed in WT embryos to validate the specific binding and signal of the Lhx6 primary antibody. Several experiments were performed to test the various dilutions of the primary antibody and whether antigen retrieval was necessary. Samples which contained the MGE, and thus should contain Lhx6-expressing cells, were chosen with reference to the Allen Developing Mouse Brain Atlas and previously published literature<sup>166</sup>. Importantly, secondary and no antibody controls were performed. In the secondary control, all steps of the IHC process were the same, except no primary antibody was added. Any signal in this condition could be autofluorescence of the tissue or non-specific binding of the secondary antibody. In the no antibody control, all the steps of the IHC process were the same, except no primary or secondary

antibody were added. Any signal in this condition is likely autofluorescence of the tissue. These controls were important to assess whether signal in the 555 nm wavelength represents specific binding of the primary antibody bound by the secondary antibody.

## MICROSCOPY

For microscopic evaluation and taking images of slides, a Leica DM16000 B inverted fluorescence microscope and LasX software were used. For all images, an exposure time of 1 second and contrast of 0.6 were used. For image processing, the software QuPath and ImageJ were used.

## RESULTS

### RAT INTRASPECIES and MOUSE INTERSPECIES CHIMERISM

Out of 111 chimeric blastocysts generated by *HHEX* KO and blastocyst complementation with rESCs in spring 2022, a total of 12 embryos survived to at least E12.5 and were collected. Of these, 7 appeared to have at least some eGFP expression by whole mount microscopy after collection (Table 1). Selected embryos were sectioned and stained with DAPI to assess broad chimerism (Figure 3).

	Embryos transferred	Embryos collected	GFP+	Apparent efficiency
rESC	111	12	7	7/111 (6.31%)
miPSC	75	10	2	2/75 (2.67%)

Table 1. Apparent chimerism efficiency following *HHEX* KO and complementation with PSCs.



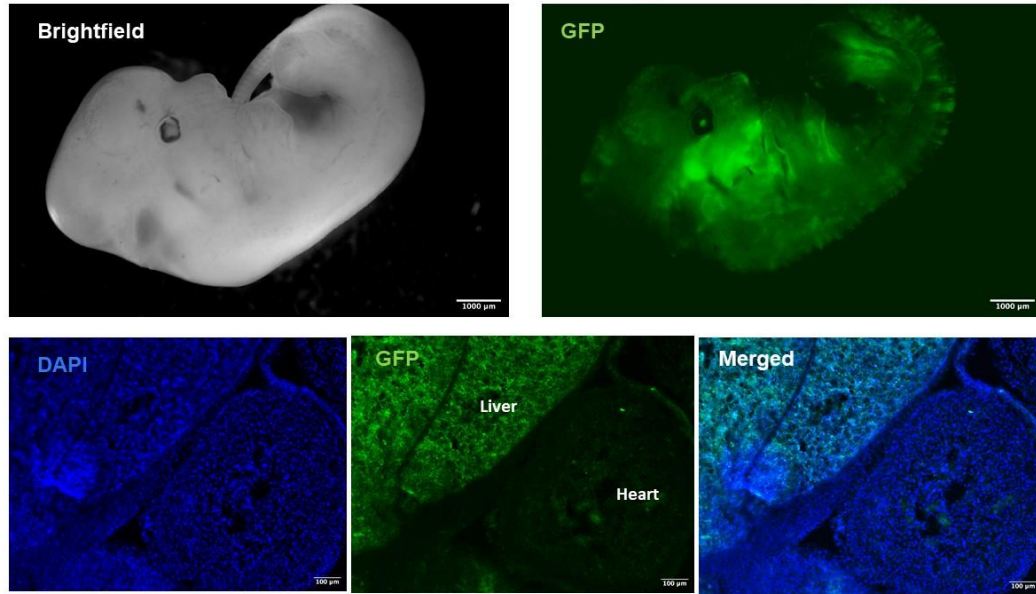


Figure 3. Chimerism in ~E12.5 *HHEX* KO/rESC complemented embryo. Upper panel – whole mount; scale bar = 1000 µm. Lower panel – chimerism indicated by strong GFP signal in liver compared to heart; scale bar = 100 µm. Image constructed in collaboration with Anala Shetty and Phoebe Strell, Low Lab.

Out of 75 chimeric blastocysts generated by *HHEX* KO and blastocyst complementation with miPSCs, a total of 10 embryos survived to the intended time point and were collected. Of these, 2 appeared to have at least some GFP expression by whole mount microscopy after collection (Table 1). Together, these data suggest that *HHEX* KO and complementation with PSCs can produce chimeras, albeit at a low rate.

#### LHX6 ANTIBODY TESTING

Prior to staining for Lhx6 in the collected chimeric tissue, the anti-Lhx6 primary antibody was first tested in WT tissue to validate the specificity of staining and optimize the IHC protocol specifications. In the first experiment, 8 coronal sections of WT E12.5 mouse were used. Antigen retrieval was performed on half of the sections to evaluate whether it was necessary to visualize specific staining. A range of primary antibody dilutions from 1:50 to 1:500 was used according to manufacturer recommendations. At the same exposure, contrast, and brightness settings, signal strength appeared comparable between different primary

antibody dilutions, broadly stronger with antigen retrieval (Figure 4B). However, the signal pattern in the slides stained with primary antibody appeared similar to the secondary control (Figure 4B), and significant overlap of the signal pattern seen in the 555 channel with the 488 channel (Figure 4C). As only the 555 secondary antibody was used, this suggested that the signal pattern was due to non-specific binding, autofluorescence of the tissue, or both. The selected sections used in the experiment may also have been from the incorrect region, as the MGE was not clearly visible. Thus, the results of the first test were inconclusive as to whether the anti-Lhx6 antibody was specifically bound and what IHC protocol specifications to use.

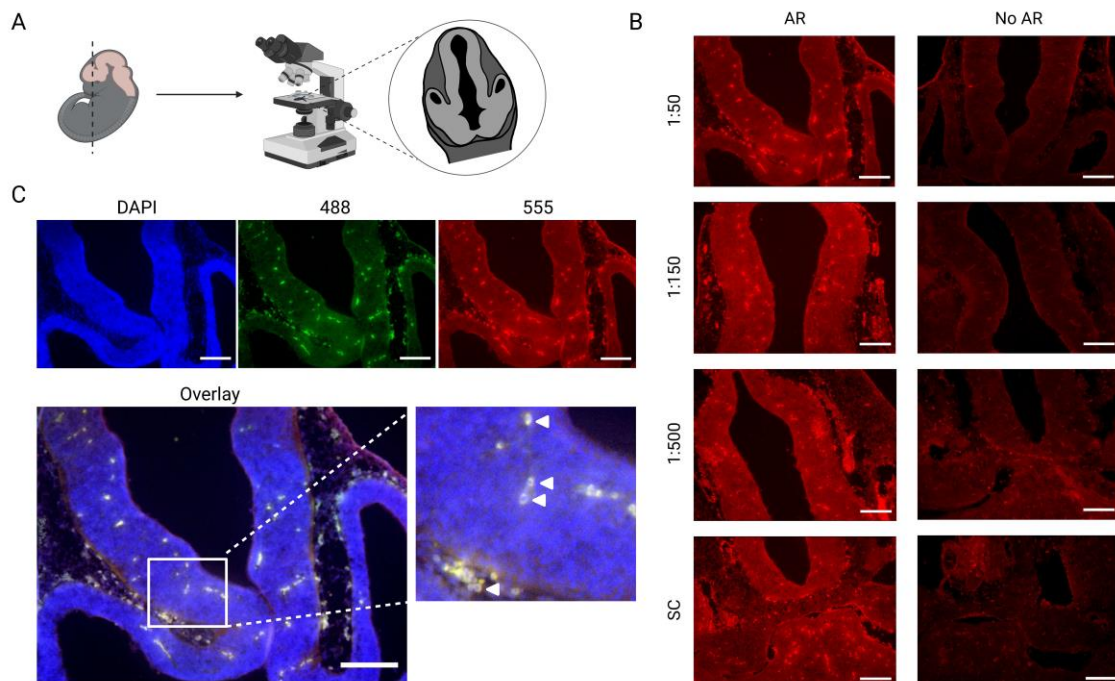


Figure 4. Results of Lhx6 antibody test 1 in coronal sections of WT E12.5 mouse brain. A) General methods. Coronal section of E12.5 mouse brain included for reference. B) Comparison of different protocols. Left panels – antigen retrieval (AR) performed. Right panels – antigen retrieval not performed. Lhx6 primary antibody was tested at 1:50, 1:150, and 1:500 dilutions. Bottom panels – secondary only control (SC). C) Comparison of DAPI, 555, and 488 channels, showing significant overlap between 488 and 555, and apparent cytoplasmic nature of signal. Examples of cells with overlapping cytoplasmic fluorescence indicated by arrows. 488 channel relative brightness increased for visual clarity. Scale bars = 200  $\mu$ m. Produced using BioRender.com.

In the second Lhx6 antibody validation experiment, 8 sagittal sections of E12.5 WT mouse were used. As the results of the first test were inconclusive, antigen retrieval was again used on half the slides. The primary antibody was tested at dilutions of 1:50 and 1:500. Secondary controls were included, and a no-antibody control was also included in this experiment with the intent to assess whether the signal seen in the first test was autofluorescence (fluorescence due to endogenous molecules), non-specific binding and fluorescence of the secondary antibody, or both. Sections were also carefully selected with reference to the Allen Developing Mouse Brain Atlas and previous literature so that they should include Lhx6+ cells. Notably, as with test 1, the same distinctive signal pattern highlighted in Figure 4B was observed in the no-antibody control (Figure 5B). This suggested this particular pattern (scattered cells with cytoplasmic fluorescence at both the 488 nm and 555 nm wavelengths) had a component of autofluorescence. A different signal pattern was observed in several samples which matched the expected specific signal pattern for Lhx6 in the brain and jaw (Figure 5C)<sup>162,171</sup>. This signal pattern was observed in slides subject to antigen retrieval, and a 1:500 dilution of the primary antibody was used. Notably, the pattern appeared to be localized to the nucleus, as the signal was pink indicating an overlap of DAPI and red fluorescence. This matches what would be expected of Lhx6 as a transcription factor. Finally, this signal pattern did not overlap with the presumed autofluorescent pattern. These results suggested the anti-Lhx6 primary antibody could successfully identify interneuron progenitors in embryonic mouse brain.

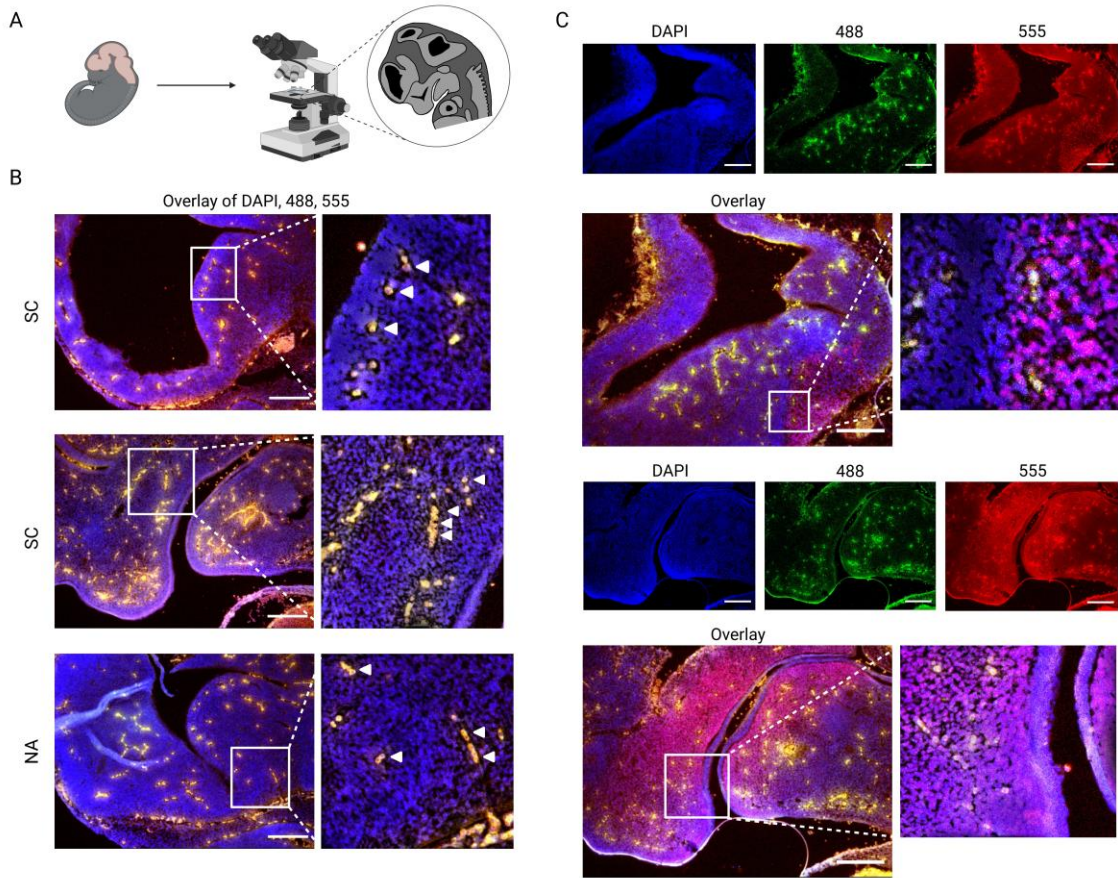


Figure 5. Results of Lhx6 antibody test 2 in sagittal sections of WT E12.5 mouse brain. A) General methods. Sagittal section of E12.5 mouse head included for reference. B) Overlays of DAPI, 555, and 488 channels for secondary (SC) and no-antibody (NA) controls, showing significant overlap between 488 and 555 and apparent cytoplasmic nature of signal, suggesting autofluorescence. Examples of cells with overlapping cytoplasmic fluorescence indicated by arrows. 488 and 555 channel relative brightness increased, background subtracted, and contrast adjusted in inset for visual clarity. C) Possible specific staining of Lhx6+ cells. Comparison of DAPI, 555, and 488 channels, showing lack of overlap between 488 and 555 and apparent nuclear nature of signal, suggesting specific Lhx6 staining. 488 channel relative brightness increased, background subtracted, and contrast adjusted in inset for visual clarity. Scale bars = 200  $\mu$ m. Produced using BioRender.com.

After promising results with Lhx6 antibody test 2, a third experiment was planned to confirm specific staining of Lhx6+ cells in the MGE. Coronal sections with defined ganglionic eminences were used. As apparent specific binding was visualized in the previous experiment with antigen retrieval and at a primary antibody dilution of 1:500, these conditions were used for all non-control slides in test 3. Similarly to test 2, a signal pattern was observed in several samples which

matched the expected signal pattern for Lhx6 and did not overlap with the presumed autofluorescent pattern (Figure 6). Notably, this signal was stronger in the subventricular zone (SVZ) compared to the ventricular zone (VZ), matching what is expected of Lhx6 at this timepoint, and what may be tangentially migrating cells can be seen in a line stretching towards the cortex (Figure 6B) <sup>162-164,172</sup>. These results support the observation in test 2 that this protocol can successfully identify Lhx6+ cells in embryonic mouse MGE.

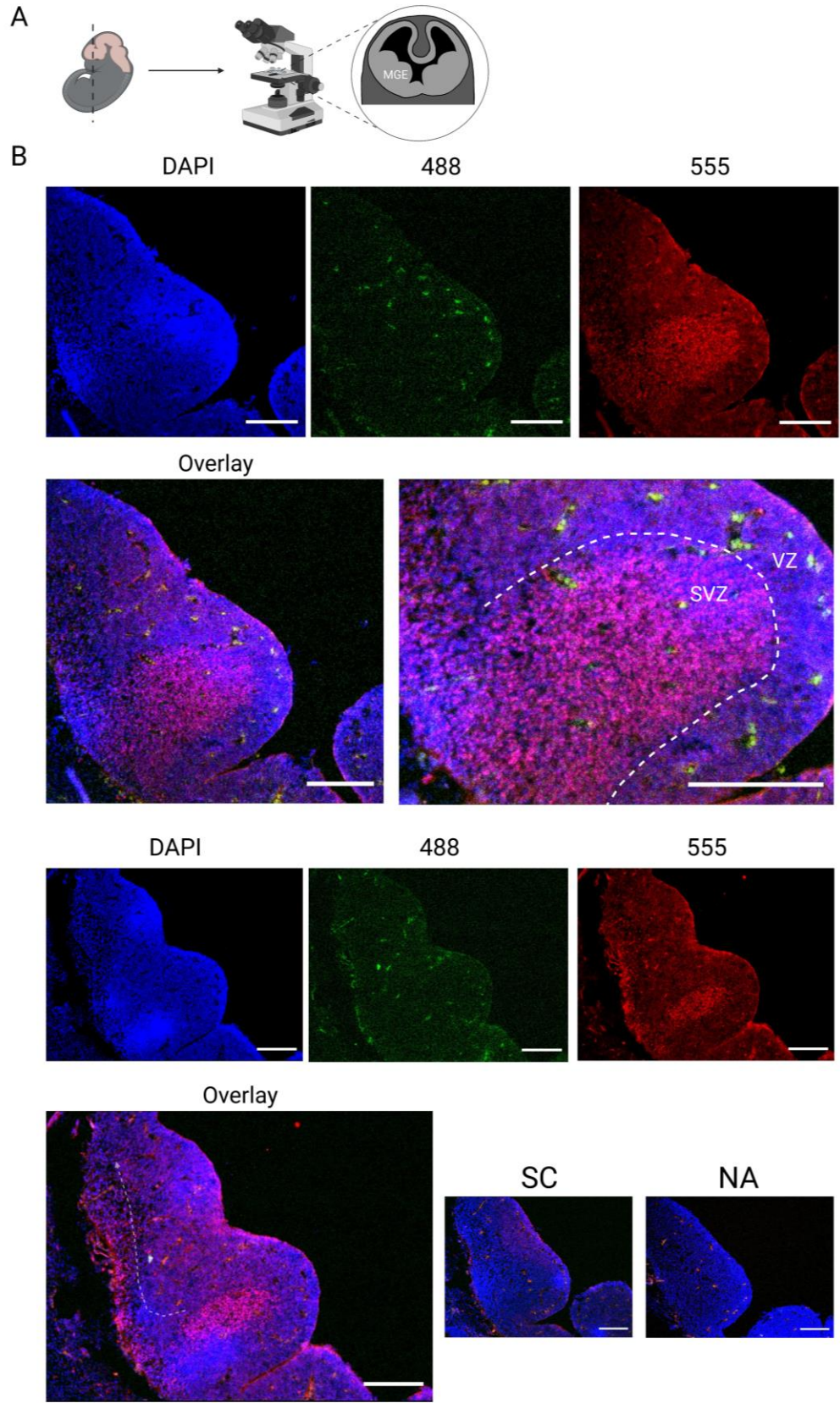


Figure 6. Results of Lhx6 antibody test 3 in coronal section of WT E12.5 mouse brain. A) General methods. Coronal section of E12.5 mouse head with MGE indicated included for reference. B) Comparison of DAPI, 555, and 488 channels, showing apparent specific Lhx6 signal lacking overlap between 488 and 555, with nuclear localization, and absent in the secondary control (SC) and no-antibody control (NA). SVZ = subventricular zone, VZ = ventricular zone. Dashed arrow represents tangential migratory path of Lhx6+ interneuron progenitors. 488 channel relative brightness increased for visual clarity. Scale bars = 200  $\mu\text{m}$ . Produced using BioRender.com.

## DISCUSSION

To this point, it appears that a protocol has been identified using the anti-Lhx6 primary antibody can successfully identify MGE interneuron progenitors in WT embryonic mouse brain. The apparent next step would be to use the same protocol to stain for Lhx6+ chimeric embryos collected which appeared GFP+. Hypothesized results of that experiment are indicated in Figure 6, indicating an overlap of GFP and Lhx6 expression in the MGE, which would suggest that the chimeric sample contained donor-derived interneuron progenitors following *HHEX* KO and complementation.

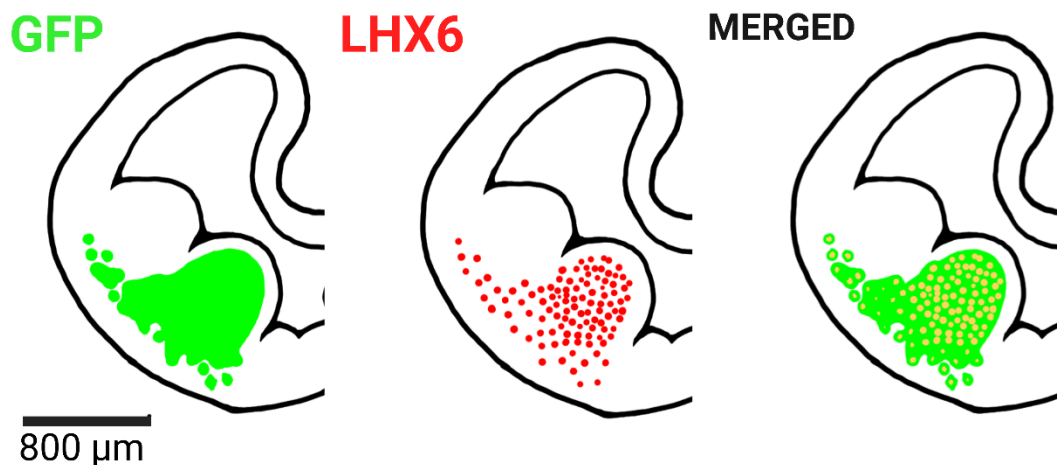


Figure 7. Hypothesized results of IHC experiments in coronal brain sections of an ~E12.5 chimeric embryo following *HHEX* KO and complementation with PSCs. Indicated is co-immunostaining of GFP (expressed in cells derived from donor PSC) and Lhx6 in the MGE. This result would suggest that this embryo had interneuron progenitors derived from donor PSC. Produced with BioRender.com.

One caveat is that post-collection processing of the chimeric embryos, including cryosectioning and the results of genotyping, has yet to be completed.

Genotyping may indicate that *HHEX* KO was unsuccessful and or provide evidence that there are no GFP+ cells in collected embryos. In that case, the knockout and complementation processes will need to be refined and performed again to generate animals which are “true” complemented chimeras. Due to the low success rate using rESC in spring 2022, complementation experiments performed in fall 2022 were done with miPSC. The rationale for this was that



intraspecies chimerism is generally more efficient than interspecies chimerism<sup>116</sup>, and the hope was to generate more samples for use in this project and others. However, to date the success rate with miPSC intraspecies blastocyst complementation was actually lower than with rESC interspecies complementation. Further refinements to the protocol, especially ensuring successful *HHEX* KO and improving the survival of KO/complemented embryos through the transfer process, are needed.

Further experiments may also be performed in WT tissue to optimize the staining protocol. As an apparent specific signal has been visualized with a 1:500 dilution of the primary antibody, further testing at lower dilutions could be performed to find the minimum dilution necessary. Additional testing with other antibodies could supply further evidence to support the identified cells as Lhx6+ interneuron progenitors. The antigen retrieval process appears beneficial for visualization of Lhx6+ cells, or at the very least, does not appear to significantly hinder the staining. Another interesting result of these tests was a significant amount of off-target signal, which appears to have components of autofluorescence and non-specific binding. A degree of non-specific binding was not unexpected given the use of a primary antibody raised in the mouse and a secondary raised against mouse, and why secondary and no-antibody controls were used. Blood cells can exhibit autofluorescence<sup>173</sup>, and the pattern seen in the tests may represent blood vessels. A literature search also identified lipofuscins, lipid containing pigment molecules, as potential sources of autofluorescence; however, as these molecules are typically found in post-mitotic cells, they may be less likely to be present in sufficient quantities at the embryonic stage<sup>174,175</sup>. Testing different blocking solutions may also enable minimization of non-specific binding in future experiments. Reagents such as TrueBlack®, which is designed to quench autofluorescence and has been tested in embryonic mouse tissue, may also be used<sup>173</sup>. Minimizing background signal will be important to distinguish GFP+ donor cells from cells with green autofluorescence in complemented samples. One potential method to distinguish GFP+ cells would be to use a primary

antibody against GFP, and a secondary antibody with fluorescence of a different wavelength than that used for HHEX.

One potential takeaway from this work is additional evidence that the gene *HHEX* is important for brain development. In previous work, *HHEX* homozygous knockout led to defects and or total loss of forebrain structures<sup>138</sup>. However, most work on *HHEX* has focused on its role in other tissues such as liver, pancreas, heart, and thyroid<sup>119,136,137,176,177</sup>. In future complementation experiments, if there is consistently a significant population of donor-derived forebrain cells, this would suggest that *HHEX* KO creates a niche in the brain, and *Hhex* is therefore important for normal brain development.

In summary, *HHEX* KO followed by blastocyst complementation with PSCs still represents a potential method to generate exogenic interneurons. Further refinements in the production of interspecies and intraspecies rodent chimeras are needed. In addition, if *HHEX* blastocyst complementation is successful in rodents, there is a possibility it may be successful with human donor cells in a pig host. An additional hypothetical experiment in the line of thinking of this project is the transplant of interneuron progenitors generated via blastocyst complementation into a mouse model of AD. Interneuron progenitor transplant for AD has been previously explored in mouse models<sup>67,97,98</sup>, and the use of blastocyst complementation to generate donor-derived MGE may overcome previously discussed challenges associated with neural cell transplant as a therapy. However, there are legitimate ethical concerns about work involving chimera, and further research in this field should be done with appropriate transparency and guidance from regulatory bodies.

## BIBLIOGRAPHY

1. 2021 Alzheimer's disease facts and figures. (2021). *Alzheimers Dement* 17, 327–406. 10.1002/alz.12328.
2. Bature, F., Guinn, B.-A., Pang, D., and Pappas, Y. (2017). Signs and symptoms preceding the diagnosis of Alzheimer's disease: a systematic scoping review of literature from 1937 to 2016. *BMJ Open* 7, e015746. 10.1136/bmjopen-2016-015746.
3. Atri, A. (2019). The Alzheimer's Disease Clinical Spectrum: Diagnosis and Management. *Med Clin North Am* 103, 263–293. 10.1016/j.mcna.2018.10.009.
4. Chen, G.-F., Xu, T.-H., Yan, Y., Zhou, Y.-R., Jiang, Y., Melcher, K., and Xu, H.E. (2017). Amyloid beta: structure, biology and structure-based therapeutic development. *Acta Pharmacol Sin* 38, 1205–1235. 10.1038/aps.2017.28.
5. Brothers, H.M., Gosztyla, M.L., and Robinson, S.R. (2018). The Physiological Roles of Amyloid- $\beta$  Peptide Hint at New Ways to Treat Alzheimer's Disease. *Frontiers in Aging Neuroscience* 10.
6. Bishop, G.M., and Robinson, S.R. (2004). Physiological Roles of Amyloid- $\beta$  and Implications for its Removal in Alzheimer's Disease. *Drugs Aging* 21, 621–630. 10.2165/00002512-200421100-00001.
7. Walker, L.C. (2020). A $\beta$  Plaques. *Free Neuropathol* 1, 31. 10.17879/freeneuropathology-2020-3025.
8. Goedert, M., Spillantini, M.G., Jakes, R., Rutherford, D., and Crowther, R.A. (1989). Multiple isoforms of human microtubule-associated protein tau: sequences and localization in neurofibrillary tangles of Alzheimer's disease. *Neuron* 3, 519–526. 10.1016/0896-6273(89)90210-9.
9. Naseri, N.N., Wang, H., Guo, J., Sharma, M., and Luo, W. (2019). The complexity of tau in Alzheimer's disease. *Neurosci Lett* 705, 183–194. 10.1016/j.neulet.2019.04.022.
10. Soria Lopez, J.A., González, H.M., and Léger, G.C. (2019). Chapter 13 - Alzheimer's disease. In *Handbook of Clinical Neurology*, S. T. Dekosky and S. Asthana, eds. (Elsevier), pp. 231–255. 10.1016/B978-0-12-804766-8.00013-3.
11. DeTure, M.A., and Dickson, D.W. (2019). The neuropathological diagnosis of Alzheimer's disease. *Molecular Neurodegeneration* 14, 32. 10.1186/s13024-019-0333-5.
12. Sengoku, R. (2020). Aging and Alzheimer's disease pathology. *Neuropathology* 40, 22–29. 10.1111/neup.12626.
13. König, T., and Stögmann, E. (2021). Genetics of Alzheimer's disease. *Wiener Medizinische Wochenschrift* 171, 249–256. 10.1007/s10354-021-00819-9.

14. Hardy, J. (1996). New Insights into the Genetics of Alzheimer's Disease. *Annals of Medicine* 28, 255–258. 10.3109/07853899609033127.
15. Guerreiro, R., and Hardy, J. (2014). Genetics of Alzheimer's Disease. *Neurotherapeutics* 11, 732–737. 10.1007/s13311-014-0295-9.
16. Huang, Y.-W.A., Zhou, B., Wernig, M., and Südhof, T.C. (2017). ApoE2, ApoE3, and ApoE4 Differentially Stimulate APP Transcription and A $\beta$  Secretion. *Cell* 168, 427-441.e21. 10.1016/j.cell.2016.12.044.
17. Guerreiro, R., Wojtas, A., Bras, J., Carrasquillo, M., Rogaeva, E., Majounie, E., Cruchaga, C., Sassi, C., Kauwe, J.S.K., Younkin, S., et al. (2013). TREM2 variants in Alzheimer's disease. *N Engl J Med* 368, 117–127. 10.1056/NEJMoa1211851.
18. Colonna, M., and Wang, Y. (2016). TREM2 variants: new keys to decipher Alzheimer disease pathogenesis. *Nat Rev Neurosci* 17, 201–207. 10.1038/nrn.2016.7.
19. Qazi, T.J., Quan, Z., Mir, A., and Qing, H. (2018). Epigenetics in Alzheimer's Disease: Perspective of DNA Methylation. *Mol Neurobiol* 55, 1026–1044. 10.1007/s12035-016-0357-6.
20. Bellenguez, C., Küçükali, F., Jansen, I.E., Kleindam, L., Moreno-Grau, S., Amin, N., Naj, A.C., Campos-Martin, R., Grenier-Boley, B., Andrade, V., et al. (2022). New insights into the genetic etiology of Alzheimer's disease and related dementias. *Nat Genet* 54, 412–436. 10.1038/s41588-022-01024-z.
21. Rasmussen, K.L., Nordestgaard, B.G., Frikke-Schmidt, R., and Nielsen, S.F. (2018). An updated Alzheimer hypothesis: Complement C3 and risk of Alzheimer's disease-A cohort study of 95,442 individuals. *Alzheimers Dement* 14, 1589–1601. 10.1016/j.jalz.2018.07.223.
22. Escott-Price, V., Myers, A.J., Huentelman, M., and Hardy, J. (2017). Polygenic risk score analysis of pathologically confirmed Alzheimer disease. *Ann Neurol* 82, 311–314. 10.1002/ana.24999.
23. A Armstrong, R. (2019). Risk factors for Alzheimer's disease. *Folia Neuropathol* 57, 87–105. 10.5114/fn.2019.85929.
24. Wong, W. (2020). Economic burden of Alzheimer disease and managed care considerations. *Am J Manag Care* 26, S177–S183. 10.37765/ajmc.2020.88482.
25. Silvestro, S., Valeri, A., and Mazzon, E. (2022). Aducanumab and Its Effects on Tau Pathology: Is This the Turning Point of Amyloid Hypothesis? *International Journal of Molecular Sciences* 23, 2011. 10.3390/ijms23042011.
26. Marucci, G., Buccioni, M., Ben, D.D., Lambertucci, C., Volpini, R., and Amenta, F. (2021). Efficacy of acetylcholinesterase inhibitors in Alzheimer's disease. *Neuropharmacology* 190, 108352. 10.1016/j.neuropharm.2020.108352.

27. Mullard, A. (2021). More Alzheimer's drugs head for FDA review: what scientists are watching. *Nature* 599, 544–545. 10.1038/d41586-021-03410-9.
28. Simić, G., Kostović, I., Winblad, B., and Bogdanović, N. (1997). Volume and number of neurons of the human hippocampal formation in normal aging and Alzheimer's disease. *J Comp Neurol* 379, 482–494. 10.1002/(sici)1096-9861(19970324)379:4<482::aid-cne2>3.0.co;2-z.
29. Rao, Y.L., Ganaraja, B., Murlimanju, B.V., Joy, T., Krishnamurthy, A., and Agrawal, A. (2022). Hippocampus and its involvement in Alzheimer's disease: a review. *3 Biotech* 12, 55. 10.1007/s13205-022-03123-4.
30. Stranahan, A.M., and Mattson, M.P. (2010). Selective vulnerability of neurons in layer II of the entorhinal cortex during aging and Alzheimer's disease. *Neural Plast* 2010, 108190. 10.1155/2010/108190.
31. Olajide, O.J., Suvanto, M.E., and Chapman, C.A. (2021). Molecular mechanisms of neurodegeneration in the entorhinal cortex that underlie its selective vulnerability during the pathogenesis of Alzheimer's disease. *Biology Open* 10, bio056796. 10.1242/bio.056796.
32. Kesner, R.P., Crutcher, K.A., and Measom, M.O. (1986). Medial septal and nucleus basalis magnocellularis lesions produce order memory deficits in rats which mimic symptomatology of Alzheimer's disease. *Neurobiol Aging* 7, 287–295. 10.1016/0197-4580(86)90009-6.
33. Lyness, S.A., Zarow, C., and Chui, H.C. (2003). Neuron loss in key cholinergic and aminergic nuclei in Alzheimer disease: a meta-analysis. *Neurobiology of Aging* 24, 1–23. 10.1016/S0197-4580(02)00057-X.
34. Whitehouse, P.J., Price, D.L., Clark, A.W., Coyle, J.T., and DeLong, M.R. (1981). Alzheimer disease: evidence for selective loss of cholinergic neurons in the nucleus basalis. *Ann Neurol* 10, 122–126. 10.1002/ana.410100203.
35. Klein-Koerkamp, Y., A. Heckemann, R., T. Ramdeen, K., Moreaud, O., Keignart, S., Krainik, A., Hammers, A., Baciú, M., Hot, P., and Alzheimer's Disease Neuroimaging Initiative, for the (2014). Amygdalar Atrophy in Early Alzheimer's Disease. *Current Alzheimer Research* 11, 239–252.
36. Wright, C.I., Dickerson, B.C., Feczko, E., Negeira, A., and Williams, D. (2007). A Functional Magnetic Resonance Imaging Study of Amygdala Responses to Human Faces in Aging and Mild Alzheimer's Disease. *Biological Psychiatry* 62, 1388–1395. 10.1016/j.biopsych.2006.11.013.
37. Trillo, L., Das, D., Hsieh, W., Medina, B., Moghadam, S., Lin, B., Dang, V., Sanchez, M.M., De Miguel, Z., Ashford, J.W., et al. (2013). Ascending monoaminergic systems alterations in Alzheimer's disease. Translating basic science into clinical care. *Neuroscience & Biobehavioral Reviews* 37, 1363–1379. 10.1016/j.neubiorev.2013.05.008.

38. Matchett, B.J., Grinberg, L.T., Theofilas, P., and Murray, M.E. (2021). The mechanistic link between selective vulnerability of the locus coeruleus and neurodegeneration in Alzheimer's disease. *Acta Neuropathol* 141, 631–650. 10.1007/s00401-020-02248-1.
39. Theofilas, P., Ehrenberg, A.J., Dunlop, S., Di Lorenzo Alho, A.T., Nguy, A., Leite, R.E.P., Rodriguez, R.D., Mejia, M.B., Suemoto, C.K., Ferretti-Rebustini, R.E.D.L., et al. (2017). Locus coeruleus volume and cell population changes during Alzheimer's disease progression: A stereological study in human postmortem brains with potential implication for early-stage biomarker discovery. *Alzheimer's & Dementia* 13, 236–246. 10.1016/j.jalz.2016.06.2362.
40. Strell, Phoebe, Johnson, Sether T, Carchi, Chris, and Low, Walter C Prospects for Generating Exogenic Neurons for Treating Alzheimer's Disease. *Cell Transplantation Submitted for review.*
41. Theibert, A.B. (2020). Organization & Cells of the Nervous System. In *Essentials of Modern Neuroscience*, F. R. Amthor, A. B. Theibert, D. G. Standaert, and E. D. Roberson, eds. (McGraw Hill).
42. Lim, L., Mi, D., Llorca, A., and Marín, O. (2018). Development and Functional Diversification of Cortical Interneurons. *Neuron* 100, 294–313. 10.1016/j.neuron.2018.10.009.
43. Kepecs, A., and Fishell, G. (2014). Interneuron cell types are fit to function. *Nature* 505, 318–326. 10.1038/nature12983.
44. Fishell, G., and Kepecs, A. (2020). Interneuron Types as Attractors and Controllers. *Annu Rev Neurosci* 43, 1–30. 10.1146/annurev-neuro-070918-050421.
45. Nahar, L., Delacroix, B.M., and Nam, H.W. (2021). The Role of Parvalbumin Interneurons in Neurotransmitter Balance and Neurological Disease. *Front Psychiatry* 12, 679960. 10.3389/fpsy.2021.679960.
46. Vargova, G., Vogels, T., Kostecka, Z., and Hromadka, T. (2018). Inhibitory interneurons in Alzheimer's disease. *Bratisl Lek Listy* 119, 205–209. 10.4149/BLL\_2018\_038.
47. Tremblay, R., Lee, S., and Rudy, B. (2016). GABAergic Interneurons in the Neocortex: From Cellular Properties to Circuits. *Neuron* 91, 260–292. 10.1016/j.neuron.2016.06.033.
48. Palop, J.J., and Mucke, L. (2016). Network abnormalities and interneuron dysfunction in Alzheimer disease. *Nat Rev Neurosci* 17, 777–792. 10.1038/nrn.2016.141.
49. Ruden, J.B., Dugan, L.L., and Konradi, C. (2021). Parvalbumin interneuron vulnerability and brain disorders. *Neuropsychopharmacology* 46, 279–287. 10.1038/s41386-020-0778-9.
50. Verret, L., Mann, E.O., Hang, G.B., Barth, A.M.I., Cobos, I., Ho, K., Devidze, N., Masliah, E., Kreitzer, A.C., Mody, I., et al. (2012). Inhibitory Interneuron Deficit Links Altered Network Activity and Cognitive Dysfunction in Alzheimer Model. *Cell* 149, 708–721. 10.1016/j.cell.2012.02.046.

51. Reid, H.M.O., Chen-Mack, N., Snowden, T., and Christie, B.R. (2021). Understanding Changes in Hippocampal Interneurons Subtypes in the Pathogenesis of Alzheimer's Disease: A Systematic Review. *Brain Connectivity* 11, 159–179. 10.1089/brain.2020.0879.
52. Giesers, N.K., and Wirths, O. (2020). Loss of Hippocampal Calretinin and Parvalbumin Interneurons in the 5XFAD Mouse Model of Alzheimer's Disease. *ASN Neuro* 12, 1759091420925356. 10.1177/1759091420925356.
53. Sekiguchi, M., Zushida, K., Yoshida, M., Maekawa, M., Kamichi, S., Yoshida, M., Sahara, Y., Yuasa, S., Takeda, S., and Wada, K. (2009). A deficit of brain dystrophin impairs specific amygdala GABAergic transmission and enhances defensive behaviour in mice. *Brain* 132, 124–135. 10.1093/brain/awn253.
54. Mahar, I., Albuquerque, M.S., Mondragon-Rodriguez, S., Cavanagh, C., Davoli, M.A., Chabot, J.-G., Williams, S., Mechawar, N., Quirion, R., and Krantic, S. (2017). Phenotypic Alterations in Hippocampal NPY- and PV-Expressing Interneurons in a Presymptomatic Transgenic Mouse Model of Alzheimer's Disease. *Frontiers in Aging Neuroscience* 8.
55. Grouselle, D., Winsky-Sommerer, R., David, J.P., Delacourte, A., Dournaud, P., and Epelbaum, J. (1998). Loss of somatostatin-like immunoreactivity in the frontal cortex of Alzheimer patients carrying the apolipoprotein epsilon 4 allele. *Neuroscience Letters* 255, 21–24. 10.1016/S0304-3940(98)00698-3.
56. Davies, P., Katzman, R., and Terry, R.D. (1980). Reduced somatostatin-like immunoreactivity in cerebral cortex from cases of Alzheimer disease and Alzheimer senile dementia. *Nature* 288, 279–280. 10.1038/288279a0.
57. Andrews-Zwilling, Y., Bien-Ly, N., Xu, Q., Li, G., Bernardo, A., Yoon, S.Y., Zwilling, D., Yan, T.X., Chen, L., and Huang, Y. (2010). Apolipoprotein E4 Causes Age- and Tau-Dependent Impairment of GABAergic Interneurons, Leading to Learning and Memory Deficits in Mice. *J. Neurosci.* 30, 13707–13717. 10.1523/JNEUROSCI.4040-10.2010.
58. Zheng, J., Li, H.-L., Tian, N., Liu, F., Wang, L., Yin, Y., Yue, L., Ma, L., Wan, Y., and Wang, J.-Z. (2020). Interneuron Accumulation of Phosphorylated tau Impairs Adult Hippocampal Neurogenesis by Suppressing GABAergic Transmission. *Cell Stem Cell* 26, 331-345.e6. 10.1016/j.stem.2019.12.015.
59. Xu, Y., Zhao, M., Han, Y., and Zhang, H. (2020). GABAergic Inhibitory Interneuron Deficits in Alzheimer's Disease: Implications for Treatment. *Front Neurosci* 14, 660. 10.3389/fnins.2020.00660.
60. Busche, M.A., Eichhoff, G., Adelsberger, H., Abramowski, D., Wiederhold, K.-H., Haass, C., Staufenbiel, M., Konnerth, A., and Garaschuk, O. (2008). Clusters of Hyperactive Neurons Near Amyloid Plaques in a Mouse Model of Alzheimer's Disease. *Science* 321, 1686–1689. 10.1126/science.1162844.
61. Amatniek, J.C., Hauser, W.A., DelCastillo-Castaneda, C., Jacobs, D.M., Marder, K., Bell, K., Albert, M., Brandt, J., and Stern, Y. (2006). Incidence and predictors of seizures in patients with Alzheimer's disease. *Epilepsia* 47, 867–872. 10.1111/j.1528-1167.2006.00554.x.

62. Palop, J.J., Chin, J., Roberson, E.D., Wang, J., Thwin, M.T., Bien-Ly, N., Yoo, J., Ho, K.O., Yu, G.-Q., Kreitzer, A., et al. (2007). Aberrant excitatory neuronal activity and compensatory remodeling of inhibitory hippocampal circuits in mouse models of Alzheimer's disease. *Neuron* 55, 697–711. 10.1016/j.neuron.2007.07.025.
63. Jia, X., and Kohn, A. (2011). Gamma rhythms in the brain. *PLoS Biol* 9, e1001045. 10.1371/journal.pbio.1001045.
64. Thompson, L., Khuc, J., Sacconi, M.S., Zokaei, N., and Cappelletti, M. (2021). Gamma oscillations modulate working memory recall precision. *Exp Brain Res* 239, 2711–2724. 10.1007/s00221-021-06051-6.
65. Barker, B.S., Young, G.T., Soubrane, C.H., Stephens, G.J., Stevens, E.B., and Patel, M.K. (2017). Chapter 2 - Ion Channels. In *Conn's Translational Neuroscience*, P. M. Conn, ed. (Academic Press), pp. 11–43. 10.1016/B978-0-12-802381-5.00002-6.
66. Corbett, B.F., Leiser, S.C., Ling, H.-P., Nagy, R., Breyse, N., Zhang, X., Hazra, A., Brown, J.T., Randall, A.D., Wood, A., et al. (2013). Sodium channel cleavage is associated with aberrant neuronal activity and cognitive deficits in a mouse model of Alzheimer's disease. *J Neurosci* 33, 7020–7026. 10.1523/JNEUROSCI.2325-12.2013.
67. Martinez-Losa, M., Tracy, T.E., Ma, K., Verret, L., Clemente-Perez, A., Khan, A.S., Cobos, I., Ho, K., Gan, L., Mucke, L., et al. (2018). Nav1.1-Overexpressing Interneuron Transplants Restore Brain Rhythms and Cognition in a Mouse Model of Alzheimer's Disease. *Neuron* 98, 75-89.e5. 10.1016/j.neuron.2018.02.029.
68. Williams, R.H., and Riedemann, T. (2021). Development, Diversity, and Death of MGE-Derived Cortical Interneurons. *Int J Mol Sci* 22, 9297. 10.3390/ijms22179297.
69. Yang, J., Yang, X., and Tang, K. (2022). Interneuron development and dysfunction. *FEBS J* 289, 2318–2336. 10.1111/febs.15872.
70. Alvarez-Dolado, M., Calcagnotto, M.E., Karkar, K.M., Southwell, D.G., Jones-Davis, D.M., Estrada, R.C., Rubenstein, J.L.R., Alvarez-Buylla, A., and Baraban, S.C. (2006). Cortical Inhibition Modified by Embryonic Neural Precursors Grafted into the Postnatal Brain. *J Neurosci*. 26, 7380–7389. 10.1523/JNEUROSCI.1540-06.2006.
71. Flames, N., Pla, R., Gelman, D.M., Rubenstein, J.L.R., Puellas, L., and Marín, O. (2007). Delineation of Multiple Subpallial Progenitor Domains by the Combinatorial Expression of Transcriptional Codes. *J. Neurosci*. 27, 9682–9695. 10.1523/JNEUROSCI.2750-07.2007.
72. Southwell, D.G., Froemke, R.C., Alvarez-Buylla, A., Stryker, M.P., and Gandhi, S.P. (2010). Cortical Plasticity Induced by Inhibitory Neuron Transplantation. *Science* 327, 1145–1148. 10.1126/science.1183962.
73. Chohan, M.O., and Moore, H. (2016). Interneuron Progenitor Transplantation to Treat CNS Dysfunction. *Frontiers in Neural Circuits* 10.



74. Li, D., Wu, Q., and Han, X. (2022). Application of Medial Ganglionic Eminence Cell Transplantation in Diseases Associated With Interneuron Disorders. *Frontiers in Cellular Neuroscience* *16*.
75. Wichterle, H., Garcia-Verdugo, J.M., Herrera, D.G., and Alvarez-Buylla, A. (1999). Young neurons from medial ganglionic eminence disperse in adult and embryonic brain. *Nat Neurosci* *2*, 461–466. 10.1038/8131.
76. Wichterle, H., Alvarez-Dolado, M., Erskine, L., and Alvarez-Buylla, A. (2003). Permissive corridor and diffusible gradients direct medial ganglionic eminence cell migration to the neocortex. *Proceedings of the National Academy of Sciences* *100*, 727–732. 10.1073/pnas.242721899.
77. Howard, M.A., and Baraban, S.C. (2016). Synaptic integration of transplanted interneuron progenitor cells into native cortical networks. *Journal of Neurophysiology* *116*, 472–478. 10.1152/jn.00321.2016.
78. Hunt, R.F., Girskis, K.M., Rubenstein, J.L., Alvarez-Buylla, A., and Baraban, S.C. (2013). GABA progenitors grafted into the adult epileptic brain control seizures and abnormal behavior. *Nat Neurosci* *16*, 692–697. 10.1038/nn.3392.
79. Tyson, J.A., and Anderson, S.A. (2014). GABAergic interneuron transplants to study development and treat disease. *Trends Neurosci* *37*, 169–177. 10.1016/j.tins.2014.01.003.
80. Hsieh, J.-Y., and Baraban, S.C. (2017). Medial Ganglionic Eminence Progenitors Transplanted into Hippocampus Integrate in a Functional and Subtype-Appropriate Manner. *eNeuro* *4*, ENEURO.0359-16.2017. 10.1523/ENEURO.0359-16.2017.
81. Tanaka, D.H., Toriumi, K., Kubo, K., Nabeshima, T., and Nakajima, K. (2011). GABAergic Precursor Transplantation into the Prefrontal Cortex Prevents Phencyclidine-Induced Cognitive Deficits. *J Neurosci* *31*, 14116–14125. 10.1523/JNEUROSCI.2786-11.2011.
82. Gilani, A.I., Chohan, M.O., Inan, M., Schobel, S.A., Chaudhury, N.H., Paskewitz, S., Chuhma, N., Glickstein, S., Merker, R.J., Xu, Q., et al. (2014). Interneuron precursor transplants in adult hippocampus reverse psychosis-relevant features in a mouse model of hippocampal disinhibition. *Proceedings of the National Academy of Sciences* *111*, 7450–7455. 10.1073/pnas.1316488111.
83. Perez, S.M., and Lodge, D.J. (2013). Hippocampal interneuron transplants reverse aberrant dopamine system function and behavior in a rodent model of schizophrenia. *Mol Psychiatry* *18*, 1193–1198. 10.1038/mp.2013.111.
84. Owoc, M.S., Rubio, M.E., Brockway, B., Sadagopan, S., and Kandler, K. (2022). Embryonic medial ganglionic eminence cells survive and integrate into the inferior colliculus of adult mice. *Hearing Research* *420*, 108520. 10.1016/j.heares.2022.108520.
85. Martínez-Cerdeño, V., Noctor, S.C., Espinosa, A., Ariza, J., Parker, P., Orasji, S., Daadi, M.M., Bankiewicz, K., Alvarez-Buylla, A., and Kriegstein, A.R. (2010). Embryonic MGE

- Precursor Cells Grafted into Adult Rat Striatum Integrate and Ameliorate Motor Symptoms in 6-OHDA-Lesioned Rats. *Cell Stem Cell* 6, 238–250. 10.1016/j.stem.2010.01.004.
86. Romariz, S.A.A., Paiva, D.S., Galindo, L.T., Barnabé, G.F., Guedes, V.A., Borlongan, C.V., and Longo, B.M. (2017). Medial Ganglionic Eminence Cells Freshly Obtained or Expanded as Neurospheres Show Distinct Cellular and Molecular Properties in Reducing Epileptic Seizures. *CNS Neuroscience & Therapeutics* 23, 127–134. 10.1111/cns.12650.
  87. Hammad, M., Schmidt, S.L., Zhang, X., Bray, R., Frohlich, F., and Ghashghaei, H.T. (2015). Transplantation of GABAergic Interneurons into the Neonatal Primary Visual Cortex Reduces Absence Seizures in Stargazer Mice. *Cerebral Cortex* 25, 2970–2979. 10.1093/cercor/bhu094.
  88. Baraban, S.C., Southwell, D.G., Estrada, R.C., Jones, D.L., Sebe, J.Y., Alfaro-Cervello, C., García-Verdugo, J.M., Rubenstein, J.L.R., and Alvarez-Buylla, A. (2009). Reduction of seizures by transplantation of cortical GABAergic interneuron precursors into Kv1.1 mutant mice. *Proceedings of the National Academy of Sciences* 106, 15472–15477. 10.1073/pnas.0900141106.
  89. Calcagnotto, M.E., Ruiz, L.P., Blanco, M.M., Santos-Junior, J.G., Valente, M.F., Patti, C., Frussa-Filho, R., Santiago, M.F., Zipancic, I., Álvarez-Dolado, M., et al. (2010). Effect of neuronal precursor cells derived from medial ganglionic eminence in an acute epileptic seizure model. *Epilepsia* 51, 71–75. 10.1111/j.1528-1167.2010.02614.x.
  90. De la Cruz, E., Zhao, M., Guo, L., Ma, H., Anderson, S.A., and Schwartz, T.H. (2011). Interneuron Progenitors Attenuate the Power of Acute Focal Ictal Discharges. *Neurotherapeutics* 8, 763–773. 10.1007/s13311-011-0058-9.
  91. Zipancic, I., Calcagnotto, M.E., Piquer-Gil, M., Mello, L.E., and Álvarez-Dolado, M. (2010). Transplant of GABAergic Precursors Restores Hippocampal Inhibitory Function in a Mouse Model of Seizure Susceptibility. *Cell Transplant* 19, 549–564. 10.3727/096368910X491383.
  92. Casalia, M.L., Howard, M.A., and Baraban, S.C. (2017). Persistent seizure control in epileptic mice transplanted with gamma-aminobutyric acid progenitors. *Annals of Neurology* 82, 530–542. 10.1002/ana.25021.
  93. Henderson, K.W., Gupta, J., Tagliatela, S., Litvina, E., Zheng, X., Zandt, M.A.V., Woods, N., Grund, E., Lin, D., Royston, S., et al. (2014). Long-Term Seizure Suppression and Optogenetic Analyses of Synaptic Connectivity in Epileptic Mice with Hippocampal Grafts of GABAergic Interneurons. *J. Neurosci.* 34, 13492–13504. 10.1523/JNEUROSCI.0005-14.2014.
  94. Bráz, J.M., Sharif-Naeini, R., Vogt, D., Kriegstein, A., Alvarez-Buylla, A., Rubenstein, J.L., and Basbaum, A.I. (2012). Forebrain GABAergic Neuron Precursors Integrate into Adult Spinal Cord and Reduce Injury-Induced Neuropathic Pain. *Neuron* 74, 663–675. 10.1016/j.neuron.2012.02.033.
  95. Southwell, D.G., Seifkar, H., Malik, R., Lavi, K., Vogt, D., Rubenstein, J.L., and Sohal, V.S. (2020). Interneuron Transplantation Rescues Social Behavior Deficits without Restoring

- Wild-Type Physiology in a Mouse Model of Autism with Excessive Synaptic Inhibition. *J. Neurosci.* *40*, 2215–2227. 10.1523/JNEUROSCI.1063-19.2019.
96. Zhu, B., Eom, J., and Hunt, R.F. (2019). Transplanted interneurons improve memory precision after traumatic brain injury. *Nat Commun* *10*, 5156. 10.1038/s41467-019-13170-w.
  97. Tong, L.M., Djukic, B., Arnold, C., Gillespie, A.K., Yoon, S.Y., Wang, M.M., Zhang, O., Knoferle, J., Rubenstein, J.L.R., Alvarez-Buylla, A., et al. (2014). Inhibitory Interneuron Progenitor Transplantation Restores Normal Learning and Memory in ApoE4 Knock-In Mice without or with A $\beta$  Accumulation. *J. Neurosci.* *34*, 9506–9515. 10.1523/JNEUROSCI.0693-14.2014.
  98. Lu, M.-H., Zhao, X.-Y., Xu, D.-E., Chen, J.-B., Ji, W.-L., Huang, Z.-P., Pan, T.-T., Xue, L.-L., Wang, F., Li, Q.-F., et al. (2020). Transplantation of GABAergic Interneuron Progenitor Attenuates Cognitive Deficits of Alzheimer’s Disease Model Mice. *Journal of Alzheimer’s Disease* *75*, 245–260. 10.3233/JAD-200010.
  99. Li, G., Bien-Ly, N., Andrews-Zwilling, Y., Xu, Q., Bernardo, A., Ring, K., Halabisky, B., Deng, C., Mahley, R.W., and Huang, Y. (2009). GABAergic Interneuron Dysfunction Impairs Hippocampal Neurogenesis in Adult Apolipoprotein E4 Knockin Mice. *Cell Stem Cell* *5*, 634–645. 10.1016/j.stem.2009.10.015.
  100. Raber, J., Wong, D., Yu, G.-Q., Buttini, M., Mahley, R.W., Pitas, R.E., and Mucke, L. (2000). Apolipoprotein E and cognitive performance. *Nature* *404*, 352–354. 10.1038/35006165.
  101. Azzouni, K. (2021). Generation of MGE-like cells from human pluripotent stem cells.
  102. Ahn, S., Kim, T.-G., Kim, K.-S., and Chung, S. (2016). Differentiation of human pluripotent stem cells into Medial Ganglionic Eminence vs. Caudal Ganglionic Eminence cells. *Methods* *101*, 103–112. 10.1016/j.ymeth.2015.09.009.
  103. Nicholas, C.R., Chen, J., Tang, Y., Southwell, D.G., Chalmers, N., Vogt, D., Arnold, C.M., Chen, Y.-J.J., Stanley, E.G., Elefanty, A.G., et al. (2013). Functional Maturation of hPSC-Derived Forebrain Interneurons Requires an Extended Timeline and Mimics Human Neural Development. *Cell Stem Cell* *12*, 573–586. 10.1016/j.stem.2013.04.005.
  104. Maroof, A.M., Keros, S., Tyson, J.A., Ying, S.-W., Ganat, Y.M., Merkle, F.T., Liu, B., Goulburn, A., Stanley, E.G., Elefanty, A.G., et al. (2013). Directed Differentiation and Functional Maturation of Cortical Interneurons from Human Embryonic Stem Cells. *Cell Stem Cell* *12*, 559–572. 10.1016/j.stem.2013.04.008.
  105. Colasante, G., Lignani, G., Rubio, A., Medrihan, L., Yekhle, L., Sessa, A., Massimino, L., Giannelli, S.G., Sacchetti, S., Caiazzo, M., et al. (2015). Rapid Conversion of Fibroblasts into Functional Forebrain GABAergic Interneurons by Direct Genetic Reprogramming. *Cell Stem Cell* *17*, 719–734. 10.1016/j.stem.2015.09.002.
  106. Kim, T.-G., Yao, R., Monnell, T., Cho, J.-H., Vasudevan, A., Koh, A., Peeyush, K.T., Moon, M., Datta, D., Bolshakov, V.Y., et al. (2014). Efficient Specification of Interneurons from Human

- Pluripotent Stem Cells by Dorsoventral and Rostrocaudal Modulation. *Stem Cells* 32, 1789–1804. 10.1002/stem.1704.
107. Noakes, Z., Keefe, F., Tamburini, C., Kelly, C.M., Santos, M.C., Dunnett, S.B., Errington, A.C., and Li, M. (2019). Human Pluripotent Stem Cell-Derived Striatal Interneurons: Differentiation and Maturation In Vitro and in the Rat Brain. *Stem Cell Reports* 12, 191–200. 10.1016/j.stemcr.2018.12.014.
  108. Liu, Y., Weick, J.P., Liu, H., Krencik, R., Zhang, X., Ma, L., Zhou, G., Ayala, M., and Zhang, S.-C. (2013). Medial ganglionic eminence–like cells derived from human embryonic stem cells correct learning and memory deficits. *Nat Biotechnol* 31, 440–447. 10.1038/nbt.2565.
  109. Cunningham, M., Cho, J.-H., Leung, A., Savvidis, G., Ahn, S., Moon, M., Lee, P.K.J., Han, J.J., Azimi, N., Kim, K.-S., et al. (2014). hPSC-Derived Maturing GABAergic Interneurons Ameliorate Seizures and Abnormal Behavior in Epileptic Mice. *Cell Stem Cell* 15, 559–573. 10.1016/j.stem.2014.10.006.
  110. Upadhyay, D., Hattiangady, B., Castro, O.W., Shuai, B., Kodali, M., Attaluri, S., Bates, A., Dong, Y., Zhang, S.-C., Prockop, D.J., et al. (2019). Human induced pluripotent stem cell-derived MGE cell grafting after status epilepticus attenuates chronic epilepsy and comorbidities via synaptic integration. *Proceedings of the National Academy of Sciences* 116, 287–296. 10.1073/pnas.1814185115.
  111. Wu, J., Platero-Luengo, A., Sakurai, M., Sugawara, A., Gil, M.A., Yamauchi, T., Suzuki, K., Bogliotti, Y.S., Cuello, C., Morales Valencia, M., et al. (2017). Interspecies Chimerism with Mammalian Pluripotent Stem Cells. *Cell* 168, 473–486.e15. 10.1016/j.cell.2016.12.036.
  112. Kobayashi, T., Yamaguchi, T., Hamanaka, S., Kato-Itoh, M., Yamazaki, Y., Iбата, M., Sato, H., Lee, Y.-S., Usui, J.-I., Knisely, A.S., et al. (2010). Generation of rat pancreas in mouse by interspecific blastocyst injection of pluripotent stem cells. *Cell* 142, 787–799. 10.1016/j.cell.2010.07.039.
  113. Morata Tarifa, C., López Navas, L., Azkona, G., and Sánchez Pernaute, R. (2020). Chimeras for the twenty-first century. *Crit Rev Biotechnol* 40, 283–291. 10.1080/07388551.2019.1679084.
  114. Levine, S., and Grabel, L. (2017). The contribution of human/non-human animal chimeras to stem cell research. *Stem Cell Res* 24, 128–134. 10.1016/j.scr.2017.09.005.
  115. Le Douarin, and M, N. (1980). The ontogeny of the neural crest in avian embryo chimaeras. *Nature* 286, 663–669. 10.1038/286663a0.
  116. Wu, J., Greely, H.T., Jaenisch, R., Nakauchi, H., Rossant, J., and Belmonte, J.C.I. (2016). Stem cells and interspecies chimaeras. *Nature* 540, 51–59. 10.1038/nature20573.
  117. Tarkowski, A.K. (1961). Mouse Chimæras Developed from Fused Eggs. *Nature* 190, 857–860. 10.1038/190857a0.

118. Gardner, R.L., and Johnson, M.H. (1973). Investigation of Early Mammalian Development using Interspecific Chimaeras between Rat and Mouse. *Nature New Biology* 246, 86–89. 10.1038/newbio246086a0.
119. Ruiz-Estevez, M., Crane, A.T., Rodriguez-Villamil, P., Ongaratto, F.L., You, Y., Steevens, A.R., Hill, C., Goldsmith, T., Webster, D.A., Sherry, L., et al. (2021). Liver development is restored by blastocyst complementation of HHEX knockout in mice and pigs. *Stem Cell Res Ther* 12, 292. 10.1186/s13287-021-02348-z.
120. Xu, Y., Davidson, L., Alt, F.W., and Baltimore, D. (1996). Function of the pre-T-cell receptor alpha chain in T-cell development and allelic exclusion at the T-cell receptor beta locus. *Proc Natl Acad Sci U S A* 93, 2169–2173. 10.1073/pnas.93.5.2169.
121. Shaw, A.C., Swat, W., Davidson, L., and Alt, F.W. (1999). Induction of Ig light chain gene rearrangement in heavy chain-deficient B cells by activated Ras. *Proc Natl Acad Sci U S A* 96, 2239–2243. 10.1073/pnas.96.5.2239.
122. Bogue, C.W., Zhang, P.-X., McGrath, J., Jacobs, H.C., and Fuleihan, R.L. (2003). Impaired B cell development and function in mice with a targeted disruption of the homeobox gene *Hex*. *Proc Natl Acad Sci U S A* 100, 556–561. 10.1073/pnas.0236979100.
123. Dahl, R., Ramirez-Bergeron, D.L., Rao, S., and Simon, M.C. (2002). Spi-B can functionally replace PU.1 in myeloid but not lymphoid development. *EMBO J* 21, 2220–2230. 10.1093/emboj/21.9.2220.
124. Kojima, H., Gu, H., Nomura, S., Caldwell, C.C., Kobata, T., Carmeliet, P., Semenza, G.L., and Sitkovsky, M.V. (2002). Abnormal B lymphocyte development and autoimmunity in hypoxia-inducible factor 1alpha -deficient chimeric mice. *Proc Natl Acad Sci U S A* 99, 2170–2174. 10.1073/pnas.052706699.
125. Liégeois, N.J., Horner, J.W., and DePinho, R.A. (1996). Lens complementation system for the genetic analysis of growth, differentiation, and apoptosis in vivo. *Proc Natl Acad Sci U S A* 93, 1303–1307. 10.1073/pnas.93.3.1303.
126. Müller, S.M., Terszowski, G., Blum, C., Haller, C., Anquez, V., Kuschert, S., Carmeliet, P., Augustin, H.G., and Rodewald, H.-R. (2005). Gene targeting of VEGF-A in thymus epithelium disrupts thymus blood vessel architecture. *Proc Natl Acad Sci U S A* 102, 10587–10592. 10.1073/pnas.0502752102.
127. Hamanaka, S., Umino, A., Sato, H., Hayama, T., Yanagida, A., Mizuno, N., Kobayashi, T., Kasai, M., Suchy, F.P., Yamazaki, S., et al. (2018). Generation of Vascular Endothelial Cells and Hematopoietic Cells by Blastocyst Complementation. *Stem Cell Reports* 11, 988–997. 10.1016/j.stemcr.2018.08.015.
128. Yamaguchi, T., Sato, H., Kato-Itoh, M., Goto, T., Hara, H., Sanbo, M., Mizuno, N., Kobayashi, T., Yanagida, A., Umino, A., et al. (2017). Interspecies organogenesis generates autologous functional islets. *Nature* 542, 191–196. 10.1038/nature21070.

129. Zheng, C., Hu, Y., Sakurai, M., Pinzon-Arteaga, C.A., Li, J., Wei, Y., Okamura, D., Ravoux, B., Barlow, H.R., Yu, L., et al. (2021). Cell competition constitutes a barrier for interspecies chimerism. *Nature* 592, 272–276. 10.1038/s41586-021-03273-0.
130. Zhang, H., Huang, J., Li, Z., Qin, G., Zhang, N., Hai, T., Hong, Q., Zheng, Q., Zhang, Y., Song, R., et al. (2018). Rescuing ocular development in an anophthalmic pig by blastocyst complementation. *EMBO Molecular Medicine* 10, e8861. 10.15252/emmm.201808861.
131. Matsunari, H., Watanabe, M., Hasegawa, K., Uchikura, A., Nakano, K., Umeyama, K., Masaki, H., Hamanaka, S., Yamaguchi, T., Nagaya, M., et al. (2020). Compensation of Disabled Organogeneses in Genetically Modified Pig Fetuses by Blastocyst Complementation. *Stem Cell Reports* 14, 21–33. 10.1016/j.stemcr.2019.11.008.
132. Mori, M., Furuhashi, K., Danielsson, J.A., Hirata, Y., Kakiuchi, M., Lin, C.-S., Ohta, M., Riccio, P., Takahashi, Y., Xu, X., et al. (2019). Generation of functional lungs via conditional blastocyst complementation using pluripotent stem cells. *Nat Med* 25, 1691–1698. 10.1038/s41591-019-0635-8.
133. Chang, A.N., Liang, Z., Dai, H.-Q., Chapdelaine-Williams, A.M., Andrews, N., Bronson, R.T., Schwer, B., and Alt, F.W. (2018). Neural blastocyst complementation enables mouse forebrain organogenesis. *Nature* 563, 126–130. 10.1038/s41586-018-0586-0.
134. Andersen, J., and Paşca, S.P. (2018). Absent forebrain replaced by embryonic stem cells. *Nature* 563, 44–45. 10.1038/d41586-018-06933-w.
135. Steevens, A.R., Griesbach, M.W., You, Y., Dutton, J.R., Low, W.C., and Santi, P.A. (2021). Generation of inner ear sensory neurons using blastocyst complementation in a Neurog1+/- deficient mouse. *Stem Cell Res Ther* 12, 1–12. 10.1186/s13287-021-02184-1.
136. Hunter, M.P., Wilson, C.M., Jiang, X., Cong, R., Vasavada, H., Kaestner, K.H., and Bogue, C.W. (2007). The homeobox gene Hhex is essential for proper hepatoblast differentiation and bile duct morphogenesis. *Developmental Biology* 308, 355–367. 10.1016/j.ydbio.2007.05.028.
137. Liu, Y., Kaneda, R., Leja, T.W., Subkhankulova, T., Tolmachov, O., Minchiotti, G., Schwartz, R.J., Barahona, M., and Schneider, M.D. (2014). Hhex and Cer1 mediate the Sox17 pathway for cardiac mesoderm formation in embryonic stem cells. *Stem Cells* 32, 1515–1526. 10.1002/stem.1695.
138. Martinez Barbera, J.P., Clements, M., Thomas, P., Rodriguez, T., Meloy, D., Kioussis, D., and Beddington, R.S. (2000). The homeobox gene Hex is required in definitive endodermal tissues for normal forebrain, liver and thyroid formation. *Development* 127, 2433–2445. 10.1242/dev.127.11.2433.
139. Crane, A.T., Aravalli, R.N., Asakura, A., Grande, A.W., Krishna, V.D., Carlson, D.F., Cheeran, M.C.-J., Danczyk, G., Dutton, J.R., Hackett, P.B., et al. (2019). Interspecies Organogenesis for Human Transplantation. *Cell Transplant* 28, 1091–1105. 10.1177/0963689719845351.

140. Casalia, M.L., Li, T., Ramsay, H., Ross, P.J., Paredes, M.F., and Baraban, S.C. (2021). Interneuron Origins in the Embryonic Porcine Medial Ganglionic Eminence. *J. Neurosci.* *41*, 3105–3119. 10.1523/JNEUROSCI.2738-20.2021.
141. Powell, K. (2022). Hybrid brains: the ethics of transplanting human neurons into animals. *Nature* *608*, 22–25. 10.1038/d41586-022-02073-4.
142. Linaro, D., Vermaercke, B., Iwata, R., Ramaswamy, A., Libé-Philippot, B., Boubakar, L., Davis, B.A., Wierda, K., Davie, K., Poovathingal, S., et al. (2019). Xenotransplanted Human Cortical Neurons Reveal Species-Specific Development and Functional Integration into Mouse Visual Circuits. *Neuron* *104*, 972-986.e6. 10.1016/j.neuron.2019.10.002.
143. Han, X., Chen, M., Wang, F., Windrem, M., Wang, S., Shanz, S., Xu, Q., Oberheim, N.A., Bekar, L., Betstadt, S., et al. (2013). Forebrain Engraftment by Human Glial Progenitor Cells Enhances Synaptic Plasticity and Learning in Adult Mice. *Cell Stem Cell* *12*, 342–353. 10.1016/j.stem.2012.12.015.
144. Crane, A.T., Voth, J.P., Shen, F.X., and Low, W.C. (2019). Concise Review: Human-Animal Neurological Chimeras: Humanized Animals or Human Cells in an Animal? *Stem Cells* *37*, 444–452. 10.1002/stem.2971.
145. Crane, A.T., Shen, F.X., Brown, J.L., Cormack, W., Ruiz-Estevez, M., Voth, J.P., Sawai, T., Hatta, T., Fujita, M., and Low, W.C. (2020). The American Public Is Ready to Accept Human-Animal Chimera Research. *Stem Cell Reports* *15*, 804–810. 10.1016/j.stemcr.2020.08.018.
146. Kito, S., Hayao, T., Noguchi-Kawasaki, Y., Ohta, Y., Hideki, U., and Tateno, S. (2004). Improved in vitro fertilization and development by use of modified human tubal fluid and applicability of pronucleate embryos for cryopreservation by rapid freezing in inbred mice. *Comp Med* *54*, 564–570.
147. Wefers, B., Bashir, S., Rossius, J., Wurst, W., and Kühn, R. (2017). Gene editing in mouse zygotes using the CRISPR/Cas9 system. *Methods* *121–122*, 55–67. 10.1016/j.ymeth.2017.02.008.
148. Barrangou, R. (2015). The roles of CRISPR–Cas systems in adaptive immunity and beyond. *Current Opinion in Immunology* *32*, 36–41. 10.1016/j.coi.2014.12.008.
149. Barrangou, R., Fremaux, C., Deveau, H., Richards, M., Boyaval, P., Moineau, S., Romero, D.A., and Horvath, P. (2007). CRISPR Provides Acquired Resistance Against Viruses in Prokaryotes. *Science* *315*, 1709–1712. 10.1126/science.1138140.
150. Ma, Y., Zhang, L., and Huang, X. (2014). Genome modification by CRISPR/Cas9. *The FEBS Journal* *281*, 5186–5193. 10.1111/febs.13110.
151. Manghwar, H., Lindsey, K., Zhang, X., and Jin, S. (2019). CRISPR/Cas System: Recent Advances and Future Prospects for Genome Editing. *Trends in Plant Science* *24*, 1102–1125. 10.1016/j.tplants.2019.09.006.

152. Redman, M., King, A., Watson, C., and King, D. (2016). What is CRISPR/Cas9? *Arch Dis Child Educ Pract Ed* 101, 213–215. 10.1136/archdischild-2016-310459.
153. Xiao-Jie, L., Hui-Ying, X., Zun-Ping, K., Jin-Lian, C., and Li-Juan, J. (2015). CRISPR-Cas9: a new and promising player in gene therapy. *Journal of Medical Genetics* 52, 289–296. 10.1136/jmedgenet-2014-102968.
154. van Beljouw, S.P.B., Sanders, J., Rodríguez-Molina, A., and Brouns, S.J.J. (2022). RNA-targeting CRISPR–Cas systems. *Nat Rev Microbiol*, 1–14. 10.1038/s41579-022-00793-y.
155. Young, J.L., and Dean, D.A. (2015). Chapter Three - Electroporation-Mediated Gene Delivery. In *Advances in Genetics Nonviral Vectors for Gene Therapy.*, L. Huang, D. Liu, and E. Wagner, eds. (Academic Press), pp. 49–88. 10.1016/bs.adgen.2014.10.003.
156. Men, H., and Bryda, E.C. (2013). Derivation of a Germline Competent Transgenic Fischer 344 Embryonic Stem Cell Line. *PLOS ONE* 8, e56518. 10.1371/journal.pone.0056518.
157. Chambers, I., and Smith, A. (2004). Self-renewal of teratocarcinoma and embryonic stem cells. *Oncogene* 23, 7150–7160. 10.1038/sj.onc.1207930.
158. McKee, C., and Chaudhry, G.R. (2017). Advances and challenges in stem cell culture. *Colloids and Surfaces B: Biointerfaces* 159, 62–77. 10.1016/j.colsurfb.2017.07.051.
159. Ying, Q.-L., Wray, J., Nichols, J., Batlle-Morera, L., Doble, B., Woodgett, J., Cohen, P., and Smith, A. (2008). The ground state of embryonic stem cell self-renewal. *Nature* 453, 519–523. 10.1038/nature06968.
160. Van Wart, H.E. (2013). Chapter 126 - Clostridium Collagenases. In *Handbook of Proteolytic Enzymes (Third Edition)*, N. D. Rawlings and G. Salvesen, eds. (Academic Press), pp. 607–611. 10.1016/B978-0-12-382219-2.00126-5.
161. Greder, L.V., Gupta, S., Li, S., Abedin, Md.J., Sajini, A., Segal, Y., Slack, J.M.W., and Dutton, J.R. (2012). Analysis of Endogenous Oct4 Activation during iPS Cell Reprogramming Using an Inducible Oct4 Lineage Label. *Stem Cells* 30, 2596–2601. 10.1002/stem.1216.
162. Grigoriou, M., Tucker, A.S., Sharpe, P.T., and Pachnis, V. (1998). Expression and regulation of Lhx6 and Lhx7, a novel subfamily of LIM homeodomain encoding genes, suggests a role in mammalian head development. *Development* 125, 2063–2074. 10.1242/dev.125.11.2063.
163. Lavdas, A.A., Grigoriou, M., Pachnis, V., and Parnavelas, J.G. (1999). The Medial Ganglionic Eminence Gives Rise to a Population of Early Neurons in the Developing Cerebral Cortex. *J. Neurosci.* 19, 7881–7888. 10.1523/JNEUROSCI.19-18-07881.1999.
164. Christodoulou, O., Maragkos, I., Antonakou, V., and Denaxa, M. (2021). The development of MGE-derived cortical interneurons: An Lhx6 tale. *Int. J. Dev. Biol.* 66, 43–49. 10.1387/ijdb.210185md.



165. Leong, T.Y.-M., and Leong, A.S.-Y. (2007). How Does Antigen Retrieval Work? *Advances in Anatomic Pathology* 14, 129–131. 10.1097/PAP.0b013e31803250c7.
166. Liu, Z., Zhang, Z., Lindtner, S., Li, Z., Xu, Z., Wei, S., Liang, Q., Wen, Y., Tao, G., You, Y., et al. (2019). Sp9 Regulates Medial Ganglionic Eminence-Derived Cortical Interneuron Development. *Cerebral Cortex* 29, 2653–2667. 10.1093/cercor/bhy133.
167. Lee, H.-S., Yamazaki, R., Wang, D., Arthaud, S., Fort, P., DeNardo, L.A., and Luppi, P.-H. (2020). Targeted recombination in active populations as a new mouse genetic model to study sleep-active neuronal populations: Demonstration that Lhx6+ neurons in the ventral zona incerta are activated during paradoxical sleep hypersomnia. *Journal of Sleep Research* 29, e12976. 10.1111/jsr.12976.
168. Angara, K., Pai, E.L.-L., Bilinovich, S.M., Stafford, A.M., Nguyen, J.T., Li, K.X., Paul, A., Rubenstein, J.L., and Vogt, D. (2020). *Nf1* deletion results in depletion of the *Lhx6* transcription factor and a specific loss of parvalbumin+ cortical interneurons. *Proceedings of the National Academy of Sciences* 117, 6189–6195. 10.1073/pnas.1915458117.
169. Kim, D.W., Liu, K., Wang, Z.Q., Zhang, Y.S., Bathini, A., Brown, M.P., Lin, S.H., Washington, P.W., Sun, C., Lindtner, S., et al. (2021). Gene regulatory networks controlling differentiation, survival, and diversification of hypothalamic Lhx6-expressing GABAergic neurons. *Commun Biol* 4, 1–16. 10.1038/s42003-020-01616-7.
170. Kapuscinski, J. (1995). DAPI: a DNA-Specific Fluorescent Probe. *Biotechnic & Histochemistry* 70, 220–233. 10.3109/10520299509108199.
171. Zhang, Z., Gutierrez, D., Li, X., Bidlack, F., Cao, H., Wang, J., Andrade, K., Margolis, H.C., and Amendt, B.A. (2013). The LIM homeodomain transcription factor LHX6: a transcriptional repressor that interacts with pituitary homeobox 2 (PITX2) to regulate odontogenesis. *J Biol Chem* 288, 2485–2500. 10.1074/jbc.M112.402933.
172. Liodis, P., Denaxa, M., Grigoriou, M., Akufo-Addo, C., Yanagawa, Y., and Pachnis, V. (2007). Lhx6 Activity Is Required for the Normal Migration and Specification of Cortical Interneuron Subtypes. *J. Neurosci.* 27, 3078–3089. 10.1523/JNEUROSCI.3055-06.2007.
173. Whittington, N.C., and Wray, S. (2017). Suppression of Red Blood Cell Autofluorescence for Immunocytochemistry on Fixed Embryonic Mouse Tissue. *Curr Protoc Neurosci* 81, 2.28.1-2.28.12. 10.1002/cpns.35.
174. Terman, A., and Brunk, U.T. (1998). Lipofuscin: mechanisms of formation and increase with age. *APMIS* 106, 265–276. 10.1111/j.1699-0463.1998.tb01346.x.
175. Schnell, S.A., Staines, W.A., and Wessendorf, M.W. (1999). Reduction of lipofuscin-like autofluorescence in fluorescently labeled tissue. *J Histochem Cytochem* 47, 719–730. 10.1177/002215549904700601.
176. Fernández, L.P., López-Márquez, A., and Santisteban, P. (2015). Thyroid transcription factors in development, differentiation and disease. *Nat Rev Endocrinol* 11, 29–42. 10.1038/nrendo.2014.186.

177. Yang, D., Cho, H., Tayyebi, Z., Shukla, A., Luo, R., Dixon, G., Ursu, V., Stransky, S., Tremmel, D.M., Sackett, S.D., et al. (2022). CRISPR screening uncovers a central requirement for HHEX in pancreatic lineage commitment and plasticity restriction. *Nat Cell Biol* 24, 1064–1076. [10.1038/s41556-022-00946-4](https://doi.org/10.1038/s41556-022-00946-4).